β-1,6-glucan plays a central role in the structure and remodeling of the bilaminate fungal cell wall

Clara Bekirian[1], Isabel Valsecchi[2], Sophie Bachellier-Bassi[1], Cyril Scandola[3], J. Iñaki Guijarro[4], Murielle Chauvel[1], Thierry Mourer[5], Neil A.R. Gow[6], Vishukumar Aimanianda[7], Christophe d'Enfert[1] and Thierry Fontaine[1]*

[1]Institut Pasteur, Université Paris Cité, INRAE, USC2019, Unité Biologie et Pathogénicité Fongiques, F-75015 Paris, France

[2]EA DYNAMYC 7380, Faculté de Santé, Université Paris-Est Créteil (UPEC), École Nationale Vétérinaire d'Alfort (EnvA), USC Anses, 94010 Créteil, France

[3]Institut Pasteur, Université Paris Cité, Ultrastructural Bioimaging Unit, 75015 Paris, France.

[4]Institut Pasteur, Université Paris Cité, CNRS UMR3528, Biological NMR and HDX-MS Technological Platform, F-75015 Paris, France

[5]Institut Pasteur, Advanced Molecular Virology group

[6] Medical Research Council Centre for Medical Mycology, University of Exeter, Geoffrey Pope Building, Stocker Road, Exeter EX4 4QD, UK

[7]Institut Pasteur, Université Paris Cité, Immunobiology of *Aspergillus* group, Paris, France

***Corresponding author:** thierry.fontaine@pasteur.fr

Keywords: β-1,6-glucan, cell wall, *Candida albicans*, *KRE6*, immune response

Abstract

The cell wall of human fungal pathogens plays critical roles as an architectural scaffold and as a target and modulator of the host immune response. Although the cell wall of the pathogenic yeast *Candida albicans* is intensively studied, one of the major fibrillar components in its cell wall, β-1,6-glucan, has been largely neglected. Here, we show that β-1,6-glucan is essential for bilayered cell wall organization, cell wall integrity and filamentous growth. For the first time, we show that β-1,6-glucan production compensates the defect in mannan elongation in the outer layer of the cell wall. In addition, β-1,6-glucan dynamics are also coordinated by host environmental stimuli and stresses with wall remodeling, where the regulation of β-1,6-glucan structure and chain length is a crucial process. As we point out that β-1,6-glucan is exposed at the yeast surface and modulate immune response, β-1,6-glucan must be considered a key factor in host-pathogen interactions.

Introduction

Pathogenic fungi are a significant burden to public health, recently estimated to cause 2.5 million annually attributable deaths worldwide[1]. Among these, *Candida* species are responsible for more than 100 million mucosal infections and 1.5 million systemic infections, representing the fourth most frequent cause of bloodstream infection in hospitalized patients[1–3]. *Candida albicans* is the most common opportunistic species, which in healthy individuals often colonizes mucosal surfaces (oral cavity, gastrointestinal tract, as well as genital tract)[4], but leads to invasive infection, post trauma or when immune system of the host is compromised. *C. albicans* is classified in the critical priority group of the WHO list of fungal pathogens[5].

Fungal cells are enveloped by a cell wall, which is essential for protection, integrity, and to maintain cell morphology. During commensalism with human hosts, the cell wall enables fungi to survive host defenses, whereas during pathogenic interactions, the cell wall also plays a central role in the polarized growth of invasive hyphae, thereby facilitating host tissue invasion[6,7]. The cell wall architecture is dynamic and therefore critical in modulating the host immune responses[8,9], which are driven by host immune receptors (pattern recognition receptors [PRRs])[10–12]. Recognition of fungal pathogen-associated molecular patterns (PAMPs) by host PRRs triggers an array of antifungal responses, including phagocytosis, the production of reactive oxygen/nitrogen species (ROS/RNS), neutrophil extracellular traps, and the release of cytokines and chemokines that recruit immune cells to the site of infection and activate adaptive immunity[12–15]. Being extracellular, thereby first to interact with the host immune system, fungal cell wall components function as the major PAMPs.

The cell wall of *C. albicans* is a complex structure with a fibrillar outer layer of mannoproteins and an inner polysaccharide layer composed of chitin, β-1,3-glucan and β-1,6-glucan, which are not present in mammalian cells[16]. Dectin-1, a C-type lectin receptor that recognizes fungal cell wall β-1,3-glucan, has been demonstrated to play a dominant pro-inflammatory role in antifungal immunity[17–21]. Chitin particles derived from the *C. albicans* cell wall lead to the selective secretion of the anti-inflammatory cytokine IL-10[22]. Mannans from *C. albicans* are recognized by multiple receptors expressed on different immune cells (Mannose receptor, DC-SIGN, TLR4, Dectin-2, Dectin-3), which are involved in yeast phagocytosis and appear to play a critical role in the induction of Th17 responses[23,24]. *C. albicans* has developed strategies to sense environmental signals encountered within the host and to regulate the exposure of its cell wall PAMPs. For example, low levels of β-1,3-glucan exposure by *C. albicans* correlate with enhanced colonization of the gastrointestinal tract[25,26] and β-1,3-glucan is mainly hidden from immune recognition by the outer layer of mannan fibrils[11,27,28]. Although these *C. albicans* cell wall polysaccharide PAMPs have been investigated in the context of host-fungal interaction, the immunomodulatory potentials of β-1,6-glucan, another major constituent of the *C. albicans* cell wall, remains under-investigated.

The composition and organization of the fungal cell wall result from an equilibrium between syntheses and remodeling of the constituent polysaccharides[23,29]. β-glucans and chitin, which account for about 60% and 2-10% (depending on the morphotype), respectively, are cross-linked to form the skeletal armor of the *C. albicans* cell wall[15,30]. Mannoproteins, which are predominantly glycosylphosphatidylinositol (GPI)-modified and covalently linked to the skeletal polysaccharides via β-1,6-glucan bridges[30,31], account for 30%–40% of the cell wall. β-1,6-glucan is composed of a linear chain of β-1,6-linked glucose residues with few short side-chains of β-1,3-glucoside or laminaribioside residues[32,33]. According to analytical methods, the β-1,6-glucan content is highly variable, from 15 to 50%[34–37]. Although β-1,6-glucan plays a crucial structural role in the *C. albicans* cell wall, the dynamics of this cell wall polysaccharide as a function of growth or stress conditions remains underexplored.

Genes required for the full β-1,6-glucan production have been identified in model yeast, *Saccharomyces cerevisiae*[38]. Among them, *KRE5* codes a putative α-glucosyltransferase[39] (GT-24) localized in the endoplasmic reticulum (ER); its deletion results in the absence of β-1,6-glucan in *S. cerevisiae* and about 80% reduction of cell wall β-1,6-glucan content in *C. albicans*[35,40]. Functions of Kre1, Kre6, Kre9 and the related homologs are unclear. Their localization in the ER, Golgi, plasma membrane or extracellular culture medium, suggests an intracellularly initiating biosynthetic pathway of β-1,6-glucan[41,42]. *KRE6* and its functional homolog *SKN1* share 66% identity and both encode transmembrane proteins containing a glycosyl-hydrolase domain (GH-16). *KRE6* deletion in *S. cerevisiae* results in a 70% decrease in the cell wall β-1,6-glucan content[33]. In *C. albicans* the double deletion of *KRE6* and *SKN1* leads to a slow growth, cell wall abnormalities, cell separation failure, and reduced virulence[43,44]. Two more *KRE6* homologs (*KRE62* and *SKN2*) have been identified in *C. albicans*[45] but their function has not yet been investigated, and the *C. albicans* cell wall β-1,6-glucan biosynthetic pathway, namely the β-1,6-glucosyltransferase involved in β-1,6-glucan polymerization and other enzymes involved in β-1,6-glucan remodeling (elongation, branching or cross-linking with β-1,3-glucan) remains to be identified.

We standardized biochemical approaches to quantify as well as to characterize β-1,6-glucan of *C. albicans*, which allowed us to perform comparative analysis and to study the dynamic of this cell wall polysaccharide in response to stress conditions and to antifungal treatments. β-1,6-glucan biosynthesis appears to be a compensatory reaction when mannan elongation is defective, whereas the absence of β-1,6-glucan results in a significantly sick growth phenotype and complete cell wall reorganization. Moreover, β-1,6-glucan showed a distinct immunomodulatory response compared to other cell wall polysaccharides. Together, our study establishes overarching and critical roles for β-1,6-glucans in the organization, structure, biosynthesis and immunomodulatory properties of the cell wall.

Results

β-1,6-glucan - a critical polysaccharide of *C. albicans* cell wall

Despite numerous studies[34–37], the composition and organization of *C. albicans* cell wall β-1,6-glucan remain unclear. To better understand the composition and organization of the cell wall β-1,6-glucan, we have fractionated cell wall and applied new biochemical strategies to quantify and characterize them. The *C. albicans* cell wall was separated into three fractions according to polymer properties and reticulations, namely: sodium-dodecyl-sulphate-β-mercaptoethanol (SDS-β-ME) extract, alkali-insoluble (AI) and alkali-soluble (AS) fractions (see methods). In Synthetic Dextrose (SD) medium at 37°C, the SDS-β-ME fraction was the smallest (18% of total cell wall) and mainly composed of mannoproteins (Fig. 1a). The AI fraction was the major one (46%) and was exclusively composed of glucose and glucosamine, the monosaccharide building blocks of β-glucans and chitin, respectively. The AS fraction (36% of total cell wall) was characterized by a high amount of mannose residues (54% of the fraction) resulting from the release of covalently cell wall-anchored mannoproteins (Fig. 1a), and this fraction also contained glucose residues originating from β-glucans. Overall, we found that the *C. albicans* cell wall is composed of 3% of chitin, 43% of proteins/mannoproteins (27% of mannans) and 54% of β-glucans, which was in agreement with earlier studies and validated our analytic approach (Fig.1a, 1b)[46–48].

To differentiate β-1,3-glucans and β-1,6-glucans, we developed two methods, one for the AI fraction and other for the AS fraction (see methods, and Fig. S8) as β-glucan was found in both fractions. β-1,6-glucan corresponded to 23% of the total cell wall, was mainly found in the AI fraction (Fig. 1a, 1b). β-1,6-glucan in the AI fraction could be solubilised by digesting β-1,3-glucan using an endo-β-1,3-glucanase, confirming that it is covalently linked to the cell wall β-1,3-glucan as previously shown in *S. cerevisiae*[33,49]. Further, gel filtration chromatography showed that the solubilised β-1,6-glucan was eluted in a single symmetric peak with Gaussian shape showing a homogeneous polymer with an apparent molecular weight range of 18-112 kDa (Fig. 1d), and the average molecular weight was estimated to be 58 kDa. The structure of purified β-1,6-glucan was analysed by ^{1}H and ^{13}C-NMR (Table S2) and by HPAEC after endo-β-1,6-glucanase digestion (Fig. 1e). The NMR chemical shifts and coupling constants as well as the HPAEC profile of the digested products were highly comparable to those we described for *S. cerevisiae*[33], showing a similar structure: a main chain of β-1,6-glucosyl residues with side chains of β-1,3-glucosyl or β-1,3-laminaribiosyl residues. The relative intensity of the anomeric proton in NMR and HPAEC analysis after endo-β-1,6-glucanase digestion, indicated that an average of 6.4% of glucose units of the main chain is substituted and that 88-90% of the side chains is composed of a single glucose residue (Fig. 1c, 1e, Table S2). Altogether, our data showed that β-1,6-glucan is a major cell wall polymer in *C. albicans,* representing 40% of the cell wall β-glucans.

Environmental regulation of β-1,6-glucan synthesis

The composition and surface exposure of fungal cell wall polymers is dependent on environmental growth conditions[26,29]. We applied chemical assays and our biochemical approaches to enable comparative analyses of cell wall robustness in relation to β-1,6-glucan dynamics in *C. albicans*.

First, we analysed the cell wall composition in relation to cell morphotype and growth phase (exponential vs. stationary phase, yeast vs. hyphae, planktonic vs. biofilm). No significant difference was observed between cell wall β-1,6-glucan and other polymers produced during the exponential (control) and stationary phases in yeast cells (Fig. 2). In biofilms, only a slight increase of mannan content (26% vs. 20%), but no change in relative β-glucan content was observed. In contrast, the cell wall isolated from *C. albicans* hyphae was characterized by an increase in chitin content (10% vs. 3%) as previously shown[29,48,50], as well as a reduction of β-1,6-glucan (18% vs. 23%) and mannan contents (13% vs. 20%) compared to the yeast form. The decrease in β-1,6-glucan content was reflected in a reduction of the β-1,6-glucan size (43 vs. 58 kDa), demonstrating that both content and structure of β-1,6-glucan are regulated during growth and cellular morphogenesis. In addition, a higher branching rate of β-1,3-glucan of the hyphal cell wall was also observed in the AI fraction (7.3% vs. 5.3%) (Fig. S3).

We further investigated the effect on cell wall composition of environmental growth conditions, such as temperature, pH, carbon source and hypoxia, on cell wall composition (Fig. 2). Hypoxic condition (1% O_2, 5% CO_2) resulted in a slow growth but did not lead to a significant alteration of the cell wall composition. In contrast, all other tested conditions led to a modification of cell wall composition including the proportion of β-1,6-glucan. For example, growth at 30°C or in 1M NaCl led to a decrease in the cell wall β-1,6-glucan content and a decrease of β-1,6-glucan chain length. However, these decreases at low temperature were compensated by a higher content of less-branched β-1,3-glucan, whereas high salt led to an increased branching rate of both β-1,6-glucan and β-1,3-glucan (Fig. 2, Fig.S3). Buffered culture medium at pH 4 or 7.5 led to a slight decrease in the β-1,6-glucan molecular weight and an increase in its branching frequency in comparison to buffered medium at pH 5.4. However, the most pronounced alteration of the cell wall was observed in lactate containing medium, with a steep reduction of polysaccharides from the structural core, chitin (-43%), β-1,3-glucan (-48%) and mainly β-1,6-glucan (-72%), in agreement with the decrease in thickness of the inner cell wall layer previously described[51]. Lactate medium also led to a strong reduction in the average β-1,6-glucan molecular weight (19 vs. 58 kDa), a decrease of β-1,6-glucan branching (4.9 vs. 6.4%) and an increase of β-1,3-glucan branching (7.4 vs. 5.3%, Fig. S3).

The presence in the medium of short chain fatty acids (acetate, propionate, or butyrate) at physiological gut concentrations resulted in a growth defect but did not alter the global cell wall

composition. The main difference was an increase of β-1,6-glucan molecular weight (64-68 kDa vs. 58 kDa) (Fig. 2b). Oxidative stress and drugs targeting the cell wall did not induce any major alterations (Fig. 2). Cell wall chitin content was reduced in the presence of nikkomycin, a chitin synthesis inhibitor, and increased in the presence of the cell wall damaging agents Congo Red or caspofungin, as previously observed[52–54], but with no impact on β-1,3-glucan and β-1,6-glucan contents. The major stress effect we observed was in presence of caspofungin, which caused an increase of the average molecular weight of β-1,6-glucan (70 vs. 58 kDa).

These data demonstrate that the content, size, and branching of β-1,6-glucan in the *C. albicans* cell wall is regulated by numerous environmental growth and stress conditions.

β-1,6-glucan dynamics responds to alterations in inner cell wall synthesis

We investigated the dynamics of β-1,6-glucan in *C. albicans* mutants in which the genes involved in the biosynthesis or remodelling of chitin and β-1,3-glucan were deleted. Four chitin synthases, located at the plasma membrane, have been described in *C. albicans* and we have analysed three deletion mutants. Chs1 is involved in primary septum formation and is essential for vegetative growth. We therefore analyzed the conditional P_{MRP1}-*CHS1/chs1*Δ mutant under repressive condition. Chs2 is a non-essential class II enzyme and represents the major chitin synthase activity measured in cell membrane preparations[55]. Chitin synthase 3 (Chs3) is responsible for most of the cell wall chitin production and chitin ring formation at sites of cell division[56] but it is not essential for growth and viability. Our comparative analyses did not show any alteration in the chitin content in the P_{MRP1}-*CHS1/chs1*Δ and *chs2*Δ/Δ mutants, but a strong reduction was observed in the *chs3*Δ/Δ mutant (-92.3%) (Fig. S2) in accordance with previous data[57,58]. In the P_{MRP1}-*CHS1/chs1*Δ mutant, the cell wall had a 45.7% decrease in mannan content in the AS fraction and a 50% increase in β-1,6-glucan in the AI fraction (Fig. S2, Fig. 3a). In the *chs3*Δ/Δ mutant, the low proportion of chitin led to an increase of both β-1,3-glucan (x1.6) and β-1,6-glucan (x1.6) in the AS fraction (Fig. 3a, Fig. S2), suggesting a defect in β-glucans cross-linking in the cell wall polysaccharide core. No significant change in β-1,6-glucan structure was noticed for these two mutants (Fig. 3b, 3c). Strikingly, no significant effect of the *CHS2* deletion was observed on cell wall chitin content or overall wall composition.

FKS1, *FKS2* and *FKS3* encode β-1,3-glucan synthases in *C. albicans*[48,59]. As *FKS1* is essential for vegetative growth[59], we used the heterozygous *fks1*Δ mutant, which displays a haplo-insufficiency phenotype[60]. Only a decrease (-58.7%) in β-1,3-glucan content in the AS fraction (Fig. S2) was observed, without any other significant changes. Moreover, essentiality of *FKS1* prevented analysis of β-1,6-glucan dynamics in a β-1,3-glucan-deficient mutant. *PHR1* and *PHR2* encode β-1,3-glucanosyltransferases of the GH-72 family involved in β-1,3-glucan elongation and branching at the

extracellular cell wall level[61,62]. In *C. albicans* their expression is strongly pH dependent: *in vitro*, *PHR1* is expressed above pH 5.5, while *PHR2 is* expressed below pH 5.5[63]. The *phr1*Δ/Δ mutant was thus grown at pH 7.5 and *phr2*Δ/Δ at pH 5.5. As expected for both mutants, defects in GH-72 β-1,3-glucan remodelase led to a decrease in β-1,3-glucan branching (-67.3% for *phr1*Δ/Δ, -31.5% for *phr2*Δ/Δ) (Fig. S4) and a compensatory increase in the cell wall chitin content (1.5x for *phr1*Δ/Δ, and 3.7x for *phr2*Δ/Δ) (Fig. S2). No change in the cell wall β-1,3-glucan content was observed in the *phr1*Δ/Δ mutant (Fig. S2). In contrast, deletion of *PHR2* led to an increase of β-1,3-glucan content and a cross-linking defect (-31.5% estimated on the ratio β-1,3-glucan content in AS and AI fractions). Concomitantly, deletion of *PHR2* led to a reduction of cell wall β-1,6-glucan content in both AI (-58.7%) and AS (-51.3%) fractions and to a reduction of molecular weight and branching of the β-1,6-glucan chains (Fig. 3a). In the *phr1*Δ/Δ mutant, only a significant increase of the molecular weight of β-1,6-glucan chain was observed (60 vs. 50 kDa) (Fig. 3).

Taken together, these data showed that mutational disruption of chitin-synthase or β-1,3-glucan-synthase genes did not significantly alter the cell wall β-1,6-glucan structure. However, defects in chitin content led to a decrease in the cross-linking of β-glucans in the inner wall (i.e. AI Fraction) that corresponds to the effect of nikkomycin treated *C. albicans* phenotype (Fig. S1); conversely, an increase in chitin content led to more cross-linking of β-glucans as observed in the *FKS1* mutant or in the presence of caspofungin (Fig. S1 and S2). In contrast, disruption of cell wall β-1,3-glucan remodelling had a pH-dependent effect on β-1,6-glucan structure (Fig. 2 and 3).

A β-1,6-glucan mannan compensatory pathway links the regulation of the inner and outer cell wall layers

In *C. albicans*, mannosylation of cell wall proteins is required for the organization of the fibrillar outer layer of the cell wall that is composed of *N*-linked mannans[27,64]. This fibrillar layer is anchored to the polysaccharide core composed of β-1,3-glucan and chitin, via β-1,6-glucan bridges[30]. We analyzed mutants deficient in Golgi α-mannosyltransferases involved in *O*- and *N*-mannosylation. Mnt1 and Mnt2 are α-1,2-mannosyltransferases involved in catalyzing consecutive reactions in *O*-mannan elongation[23,65]. As predicted, the cell wall of the *mnt1/mnt2*Δ/Δ mutant showed minor changes in overall mannan content (Fig. 3d, Fig. S2)[65]. However, deletion of *MNT1* and *MNT2* genes led to a strong reduction of β-1,6-glucan molecular weight (18 vs. 43 kDa) and an increased branching of β-1,6-glucan chains (8.6 vs. 5.3%) (Fig. 3e, 3f). A slight increase in the β-1,3-glucan branching was also observed in the *mnt1/mnt2*Δ/Δ double mutant (Fig. S4). Overall, these data suggested that β-1,6-glucan and mannan syntheses may be coupled.

N-mannan elongation requires the activity of a set α-1,6-mannosyltransferases in the Mannan Polymerase I and II complexes for the formation of α-1,6-mannan backbone that is subsequently

modified with α-1,2- and α-1,3-mannosyltransferases that assemble the *N*-mannan side chains[23]. Och1 activity is responsible for the initial addition of α-1,6-mannose onto the relatively well conserved *N*-glycan triantennary complex of glycoproteins, and Mnn9 activity is essential for the polymerization of the α-1,6-mannose backbone. Mnn2, Mnn21, Mnn22, Mnn23, Mnn24 and Mnn26 activities are essential to the synthesis of side chains[23]. Single *och1*Δ/Δ and *mnn9*Δ/Δ mutants and the sextuple *mnn2/21/22/23/24/26*Δ/Δ mutant resulted in a major decrease in mannan content in the AS fraction (-90.4% for *och1*Δ/Δ, -88.9% for *mnn9*Δ/Δ and -87.1% for *mnn2/21/22/23/24/26*Δ/Δ) and a compensatory increase in chitin content (x3.1 for *och1*Δ/Δ, x2.5 for *mnn9*Δ/Δ and x2.5 for *mnn2/21/22/23/24/26*Δ/Δ) in the AI fraction (Fig. S2), as previously described[23]. A significant increase of cell wall β-1,3-glucan content was observed in the *mnn9*Δ/Δ and *mnn2/21/22/23/24/26*Δ/Δ mutants. There was also a significant increase in the β-1,6-glucan content (x3.2 for *och1*Δ/Δ, x2.4 for *mnn9*Δ/Δ and x2.4 for *mnn2/21/22/23/24/26*Δ/Δ respectively) concomitant with the elongation of β-1,6-glucan chains, and consequential increase in its molecular weight (Fig. 3d, 3e).

Overall, these data suggest that the β-1,6-glucan biosynthesis is stimulated via a compensatory pathway when there is a defect in *O*- and *N*-linked cell wall mannan biosynthesis. This novel compensatory response occurs by increasing the β-1,6-glucan content in *N*-mannan elongation-deficient mutants and increasing branching of shorter β-1,6-glucan chains in *O*-mannan-deficient mutants.

KRE6-family-members dependent β-1,6-glucan biosynthesis

Genes encoding proteins essential for β-1,6-glucan biosynthesis were first identified in *S. cerevisiae* as mutants resistant to Killer Toxin K1 (*KRE*)[38,66]. In addition, a range of proteins in the endoplasmic reticulum and Golgi (Cwh41, Rot2, Kre5, Kre6, Skn1) are critical for the assembly of this polymer[66]. We analyzed homologs of *CWH41*, *ROT2*, *KRE5* in *C. albicans*. These three calnexin cycle proteins are involved in glucosylation/deglucosylation of *N*-glycan in the ER[67] had a reduced amount of cell wall mannan (Fig. S2). Strong cell wall phenotypes were observed for *kre5*Δ/Δ and *rot2*Δ/Δ mutants which exhibited significant increases in the highly branched β-1,3-glucan (x1.8 for *rot2*Δ/Δ, x2.2 for *kre5*Δ/Δ) (Fig. S4), chitin (x4.2 for *rot2*Δ/Δ, x5.2 for *kre5*Δ/Δ) and a strong decrease in β-1,6-glucan in the *rot2*Δ/Δ (-68.7%) and *kre5*Δ/Δ mutants (-81.5%) (Fig. 3g and Fig. S2). In addition, the β-1,6-glucan structure was also altered in both mutants, with a decrease in the average molecular weight (15-16 kDa instead of 43 kDa for the parental strain) and a reduction in the side chain branching (-54.2% for *rot2*Δ/Δ, and -76.5% for *kre5*Δ/Δ) (Fig. 3h, 3i). *KRE1* encodes a plasma membrane protein whose function is not yet clear[68,69]. The *kre1*Δ/Δ *C. albicans* mutant exhibited a reduced molecular weight of β-1,6-glucan chains (20 kDa instead of 43 kDa in the parental strain) (Fig. 3h) but was not affected in overall cell wall composition (Fig. S2).

In *C. albicans,* the *KRE6* family is composed of four homologs: *KRE6*, *SKN1*, *KRE62* and *SKN2*. These genes encode putative trans-β-glycosylases of the GH-16 family for which no biochemical activity has been described to date[70]. To analyze the function of these four proteins in *C. albicans*, we used a transient CRISPR/Cas9 protocol to build the four single knockout mutants, the double *kre6/skn1*Δ/Δ and the quadruple *kre6*Δ/Δ*/kre62/skn2/skn1*Δ/Δ mutants. Among the single mutants, only *kre6*Δ/Δ exhibited a marked alteration in the cell wall composition (Fig. S2), with significantly lower β-1,6-glucan (-46.8%) (Fig. 3g) and mannan content (-42.8%) (Fig. S2), and higher β-1,3-glucan (x1.9) and chitin (x3.9) content. In addition, the β-1,6-glucan chain length was shorter (-50.5%) and more branched (x1.7) than in the parental strain (Fig. 3h, 3i) and β-1,3-glucan was also hyperbranched (x1.8) (Fig. S4). The *kre6/skn1*Δ/Δ mutant phenotype, β-1,6-glucan content and structure were similar to the single *kre6*Δ/Δ mutant (Fig. 3g, 3h, 3i). The quadruple *kre6/kre62/skn2/skn1*Δ/Δ mutant did not produce any measurable β-1,6-glucan (Fig. 3g, Fig. S2), which was confirmed by endo-β-1,6-glucanase digestion of the AI and AS fractions (Fig. S6). The absence of β-1,6-glucan was associated with an increased chitin content (9.5% vs. 2.5%), and highly branched β-1,3-glucan (48% vs. 20% in the parental strain) (Fig. S2, Fig. S4). Reintegration of *KRE6* under the control of the *ACT1* promoter restored the production of β-1,6-glucan with a structure similar to that of the parental strain (Fig. 3g, 3h, 3i).

Therefore, in *C. albicans,* deletion of all *KRE6* homologous genes led to the absence of β-1,6-glucan production and structural alterations of the cell wall, showing that the β-1,6-glucan biosynthetic pathway is critical to the regulation of cell wall homeostasis.

***KRE6* regulation of cell wall architecture**

The single deletions of *KRE62*, *SKN1* and *SKN2* did not affect the growth of *C. albicans* in SD medium nor drug sensitivity (Fig. 4), whereas the deletion of *KRE6* led to a significant increase in doubling time (x2.4, Fig. 4a, b). The double *kre6/skn1*Δ/Δ mutant had the same growth rate as *kre6*Δ/Δ (Fig. 4a, b). However, deletion of all genes of the *KRE6* homologs family (quadruple *kre6/kre62/skn2/skn1*Δ/Δ mutant) resulted in a stronger growth phenotype with a longer lag phase and a higher doubling time (x3.5 vs. parental strain). Cells of the quadruple *kre6/kre62/skn2/skn1*Δ/Δ mutant were bigger than the parental strain (Fig. 4d). In addition, the single *kre6*Δ/Δ and all multiple mutants aggregated in SD liquid medium and had increased sensitivity to the cell wall perturbing agents Congo Red, Calcofluor White, as well as to the chitin synthase inhibitor nikkomycin Z and the *N*-glycosylation inhibitor tunicamycin. No growth of the quadruple mutant was observed in the presence of either of these drugs. Surprisingly, caspofungin enhanced the growth of mutants bearing *KRE6* gene deletion (Fig. 4c). Among the single mutants, only *skn1*Δ/Δ was defective for filamentous growth; all multiple mutants also displayed defects in filamentous growth, and the severity of this phenotype was proportional to the number of *KRE6* homologous genes deleted (Fig. 4d). The

reintegration of *KRE6* under P_{ACT1} restored parental strain-like growth kinetics, filamentation and drug resistance (Fig. 4) and confirmed the above differences noted in the mutants of *KRE6* and *SKN1*[44].

Cell wall architecture, observed by transmission electron microscopy, showed that single *skn1*Δ/Δ, *kre62*Δ/Δ and *skn2*Δ/Δ mutants presented a bilayered structure with a classical fibrillar outer layer similar to the parental strain (Fig. 5). However, the outer layer of the *skn1*Δ/Δ and *skn2*Δ/Δ mutants was thicker than the WT (*skn1*Δ/Δ, 70 ± 12 nm; *skn2*Δ/Δ, 66 ± 12 nm vs. WT, 53 ± 10 nm). The cell wall of the *kre6*Δ/Δ and *kre6/skn1*Δ/Δ mutants had a heterogeneous and thicker inner layer (*kre6*Δ/Δ, 210 ± 89 nm; *kre6/skn1*Δ/Δ, 216 ± 68 nm vs. WT, 108 ± 23 nm) (Fig. 5). The external mannoprotein-rich fibrillar layer was absent in the quadruple *kre6/kre62/skn2/skn1*Δ/Δ mutant and the inner layer was thicker and of variable thickness (440 ± 158 nm vs. 108 ± 23 nm). A normal wall architecture was fully restored in the complemented strain.

These results demonstrate that β-1,6-glucan has a pivotal role in determining the architectural arrangement of polysaccharides in the cell wall, which in turn influences growth, drug sensitivity, cell morphology and filamentation.

β-1,6-glucan stimulates human peripheral blood mononuclear cells *in vitro*

The major cell wall polysaccharides of *C. albicans,* β-1,3-glucan, mannan, and chitin function as PAMPs, and their recognition by host PRRs trigger immune responses. Although β-1,6-glucan is one of the major constituent polysaccharide in the cell wall of *C. albicans*, its immunomodulatory potential has been understudied. We extracted β-1,6-glucan from the cell wall of the parental strain and used this to stimulate peripheral blood mononuclear cells (PBMCs) and neutrophils isolated from the whole blood samples of healthy human donors. As controls, PBMCs were stimulated with the AI fraction (composed of β-1,3-glucan, β-1,6-glucan and chitin) as well as with the periodate-oxidized AI fraction (AI-OxP) devoid of β-1,6-glucan. A protein profiler was used to identify cytokines, chemokines and acute phase proteins differentially released by PBMCs and neutrophils stimulated with the three different cell wall fractions (AI, AI-OxP and β-1,6-glucan) (Fig. S12, S13). Then, differentially stimulated cytokines, chemokines and acute phase proteins were quantified by ELISA. Fractions containing β-1,3-glucan (AI and AI-OxP fractions) induced the secretion of pro-inflammatory cytokines including IL-6, IL-1β and TNF-α, chemokines such as IL-8, MCP-1, MIP-1β and RANTES, and the complement factor C5a (an acute phase protein), but anti-inflammatory cytokine IL-10 was released in a relatively small amount (Fig. 6a). However, removal of β-1,6-glucan by periodate oxidation (AI-OxP) led to a significant decrease in the IL-8, IL-6, IL-1β, TNF-α, C5a and IL-10 released, suggesting that their stimulation was in part β-1,6-glucan dependent. Although the response was much lower than that induced by the AI fraction and AI-OxP, β-1,6-glucan activated

PBMCs and induced secretion of most cytokines and chemokines (Fig. 6a). Both AI and AI-OxP fractions stimulated neutrophils secreted IL-8 at a similar level (Fig. 6b) but purified β-1,6-glucan did not, suggesting that β-1,6-glucan and β-1,3-glucan stimulate innate immune cells in distinct ways. Because the structure of cell wall β-1,6-glucan is dependent on stress as well as environmental conditions of growth, we investigated the structure-function immune response of β-1,6-glucan from *C. albicans*. Shorter β-1,6-glucan chains (19 kDa) were purified from the cell wall of *C. albicans* cell wall grown with lactate as carbon source and larger β-1,6-glucan chains (70 kDa) were purified from cell wall produced in the presence of caspofungin (Fig. 2). Both fractions stimulated PBMCs and led to cytokine/chemokine secretion at a level similar to the control β-1,6-glucan, suggesting that β-1,6-glucan size was not a significant factor influencing the stimulation of PBMCs (Fig. S5).

Discussion

Cell wall β-1,6-glucan is a conserved constituent in most of the major human fungal pathogens including *Candida*, *Cryptococcus*, *Pneumocystis*, *Histoplasma* and *Malassezia* species [47,71,72]. The cell wall of fungal pathogens is the target of several classes of antifungal drugs and is critical for immune recognition and activation, therefore has been the subject of numerous investigations[29,47]. However, this polysaccharide has been neglected, perhaps because its analysis requires bespoke methodologies. Here, we established new biochemical tools for quantitative and comparative analysis of cell wall β-1,6-glucan dynamics and structure in *C. albicans* and used them to demonstrate that this polysaccharide is instrumental in determining the gross architecture of the fungal wall and its immune reactivity.

In SD medium at 37°C, β-1,6-glucan represents 23% of the total cell wall, with an average size of 58 kDa (Fig. 1). From our analytical data on *C. albicans* cell wall, we proposed an updated model underlining the true role of β-1,6-glucan as a major cell wall component (Fig. 7a). NMR has demonstrated that the structure of β-1,6-glucan in the yeast cell wall is similar between species[33,71], but there are variations in β-1,6-glucan content, chain length and branching. *Malassezia restricta* contains long β-1,6-glucan chains, averaging 80 kDa, whilst in *S. cerevisiae* and *C. albicans* they are moderate in size (30-60 kDa). We showed here that modulating environmental conditions induce significant changes in both cell wall structure and content. As described previously, lactate used as the sole carbon source led to a thinner inner cell wall layer and greater exposure of β-1,3-glucan[51,73]. We observe here that lactate medium also led to a marked reduction in cell wall β-1,6-glucan content and chain length (Fig. 2, Fig. 7b). Our data showed that several factors related to host niches (morphology, temperature, salinity, pH and presence of organic acids) and the presence of antifungals had a significant impact on the structure, size and branching of β-1,6-glucan (Fig. 7b). This dynamic nature of the β-1,6-glucan component of the wall (Fig. 2, Fig. S1 and Fig. S2) is as important that the regulation and structural diversity of chitin, mannan and β-1,3-glucan[64].

The dynamic regulation of mannan biosynthesis leading to structural changes in the outer mannoprotein layer of *C. albicans* is also under-investigated. *C. albicans* evolves in different environments as a commensal or pathogen[4], mainly in the gut, oral cavity, genital tract and blood. How fungal cell walls adapt to changing environments was recently been listed as one of the top five unanswered question in fungal cell surface research[74]. Our data demonstrate that in response to several environmental factors β-1,6-glucan and mannan productions are coupled. The *in vivo* importance of this novel dynamic process remains to be addressed but it could be critical in the articulation of host inflammatory responses[75,76].

Immunolabelling with an anti-β-1,6-glucan serum demonstrated that this polymer is exposed at the cell surface and is therefore accessible to receptors that stimulate human immune cells (Fig. S11 and Fig. 6). Similarly in *Pneumocystis carinii*, β-1,6-glucans are exposed to the cell surface and stimulate mouse macrophages leading to the release of TNF-α[72]. Our immunological data indicate that β-1,6-glucan is a *bona fide* fungal cell wall PAMP that activates the human immune system (Fig. 7d). Beads coated with pustulan (an insoluble linear form of β-1,6-glucan) activate neutrophils and induce massive ROS production and phagocytosis in a dectin-1-independent manner[77,78]. We observed that the absence of human serum in the culture medium led to a strong reduction of β-1,6-glucan induced cytokine secretion from PBMCs and that β-1,6-glucan bind to C3b (Fig. S14). These data are in agreement with the binding of pustulan to C3b/C3d, as described previously[77,78]. This allow us to assume that the opsonization by complement component C3 could partially mediated the recognition of β-1,6-glucan by immune cells, but needs to be validated experimentally. We observed that the size of soluble β-1,6-glucan did not alter immune stimulation *in vitro* (Fig. S5) whereas, despite its ability to bind soluble and particulate β-1,3-glucan polymers, Dectin-1 signaling is only activated by particulate β-1,3-glucans[79]. The relevance of fungal β-1,6-glucan to the global host immune response and mechanism of recognition remain to be investigated.

In *C. albicans*, β-1,3-glucan exposure is regulated by external signals such as hypoxia, carbon source or iron deprivation via the up-regulation of β-1,3-glucanase activities that lead to β-1,3-glucan masking and immune evasion[75,80,81]. Regulation of the mechanisms determining β-1,6-glucan exposure and the expression of secreted glucanases remains also unknown in *C. albicans*. The absence of β-1,6-glucan in the AI fraction led to a reduced inflammatory response (Fig. 6), suggesting that an endo-β-1,3-glucanase, such as Eng1, may enable the release of cross-linked β-1,6-glucan from the cell surface, which could attenuate the host response by pruning β-1,6-glucans that are covalently bound to β-1,3-glucans from the surface [81].

Cell wall organization in *C. albicans* depends on the cross-linking of all polymers that function as a dynamic flexible network [29,47]. Their interconnectedness means that alteration in the synthesis of one polymer can lead to a compensatory change and cell wall remodelling. Our data provides one new

example of this phenomenon – namely decrease in cell wall chitin content results in an increase of both β-1,3-glucans and β-1,6-glucans in the AS fraction of the wall. Chitin exists in the yeast cell wall in three forms: free (~40%), and crosslinked to β-1,3-glucan (40-45%) or β-1,6-glucan (15-20%) and crosslinked β-glucan-chitin forms the core fibrillar cell wall structure resistant to alkali-solubilization[29,82–84]. Therefore, a decrease in the chitin content might reduce the formation of fibrillar structure, thereby releasing the β-glucan contents into the AS-fraction. On other hand, in the *FKS1* mutant or upon caspofungin treatment, cell wall chitin and β-glucan-chitin contents were increased, which could be attributed to an upregulated *CRH1* expression due decreased β-1,3-glucan synthesis as in *FKS1* mutant[85] or due to caspofungin treatment. *CRH* family members are involved in the β-glucan-chitin crosslinking[86]. Interestingly, defects in the expression of *CHS1* that encodes an essential chitin synthase required to construct the primary septum, was also compensated by an increased content of cell wall β-1,6-glucan but not of β-1,3-glucan (Fig. 3). This suggests that Chs1 has other functions beyond septum construction, that had previously been suggested by loss of cell integrity and swelling of cells upon *CHS1* repression[87]. In *S. cerevisiae*, deletion of *GAS1*, the ortholog of *PHR1* and *PHR2*, led to a strong decrease of cross-linked β-1,6-glucan to β-1,3-glucan-chitin cell wall core[62]. Deletions of *PHR1* and *PHR2*, holding a β-1,3-glucan remodelling activity, led to an increased chitin content (Fig. S2) and to a reduction of β-1,3-glucan branching (Fig. S4). However, a decrease in β-1,6-glucan content and β-1,6-glucan size was only observed in the *PHR2* mutant (Fig. 3). As *PHR1* and *PHR2* genes are strongly regulated by external pH, the compensatory differences we described may be explained by pH dependent regulation of β-1,6-glucan synthesis (Fig. 3).

In *C. albicans*, the mannan moieties of glycoproteins are covalently cross-linked to the β-glucan-chitin core. Mutants defective in *N*-mannan elongation led to a marked increase in β-1,6-glucan content and size (Fig. 3). In yeast, Och1 and Mnn9 are α-1,6-mannosyltransferases that are involved in initial steps of α-1,6-mannan polymerization in the Golgi. Members of the Mnn2 α-1,2 mannosyltransferases are required for the addition of the side chains of the α-1,6-mannan backbone[23]. Mutants in these genes led to defects in the outer fibrillar layer[27,88] and increased β-1,3-glucan exposure[23,89]. The quantification of β-1,6-glucan content in these *N*-mannan deficient mutants had not been described previously in *C. albicans*[23,88] and underline the new finding that the regulation of mannan, β-glucans and chitin synthesis is coordinated and coupled. Screening with K1 toxin killer revealed a hypersensitivity of the Sc*mnn9* mutant and an increase in β-1,6-glucan cell wall content[90] reinforcing the hypothesis that β-1,6-glucans play a compensatory role when *N*-mannosylation is compromised (Fig. 7c). Thus, a defect in the fibrillar outer mannan layer led to an increase in the inner cell wall chitin and β-1,6-glucan contents (Fig. S2), suggesting their synthesis was regulated by a rescue mechanism associated with the reprogramming of specific transcriptional responses via the cell wall integrity (CWI) pathway[91]. Defects in *O*-mannosylation also affected β-1,6-glucan synthesis leading to shortened highly branched β-1,6-glucan chains, without significant changes in

overall cell wall composition, suggesting a specific inhibition of the elongation of β-1,6-glucan chain and showing that size and branching of β-1,6-glucan can be regulated independently (Fig. 7c).

Fine details of the biosynthetic pathway of yeast β-1,6-glucans are not clear. In *S. cerevisiae*, deletion of *KRE5* and *ROT2* led to a reduction in cell wall β-1,6-glucans[66]. In *C. albicans*, this reduction is characterized by the presence of short seldom-branched β-1,6-glucan chains (Fig. 3). Although no difference was observed in the *CWH41* mutant, our data imply that canonical *N*-glycan processing in the ER is required for complete β-1,6-glucan synthesis[90], and that Kre5p is not the β-1,6-glucan polymerase[35]. Furthermore, our results confirm that the β-1,6-glucan biosynthetic pathway is similar in these phylogenetically distant yeasts, and that the *N*-glycosylation pathway is critical for β-1,6-glucan synthesis. Defects in early *N*-glycan synthesis at the ER level led to concomitant defects in β-1,6-glucan synthesis while defects in *N*-mannan elongation led to increased β-1,6-glucan synthesis. However, as Kre5, Rot2 and Cwh41 are part of the calnexin cycle involved in the control of N-glycoprotein folding in the ER, early N-glycan synthesis may have an indirect effect in ensuring the functionality of the enzymes rather than the synthesis of N-glycan moiety required for β-1,6-glucan synthesis. Our hypothesis is that this biosynthesis begins intracellularly. According to *in vitro* systems in *S. cerevisiae*, the initial step is the polymerization of a linear chain by a β-glucosyltransferase using UDP-glucose as the sugar donor[33,92] and probably an as yet unknown acceptor (Fig. S15). The second step would be the addition of glucoside and laminaribioside as a side chain. Finally, after release into the cell wall, β-1,6-glucan will be cross-linked to the other cell wall polymers. Among the *KRE* genes, only *KRE6* may be directly involved in β-1,6-glucan synthesis. Kre6 and its homologs contain a β-glycosyl-hydrolase domain of the GH-16 family, which includes a large number of fungal enzymes such as Crh1 homologs that are involved in the cross-linking of chitin and β-1,3-glucan[86]. In *C. albicans*, the quadruple deletion of *KRE6*, *SKN1*, *SKN2* and *KRE62*, led to the complete absence of β-1,6-glucan in the cell wall (Fig. 3, Fig. 7e) but also in culture supernatants and in intracellular extracts (not shown), demonstrating a stop of β-1,6-glucan synthesis rather than miss-localization. The absence of β-1,6-glucan in the quadruple mutant led to global cell wall remodeling and the absence of the outer fibrillar *N*-mannan layer (Fig. 5 and Fig. 7e). Kre6 had the dominant role and its absence led to a hypersensitivity to cell wall-targeting antifungal drugs[34,44]. One exception was observed for caspofungin which enhanced the growth of all *KRE6* deleted mutants (Fig. 4c). Growth above the MIC (paradoxical growth) has been described at high caspofungin concentrations and is associated with high chitin content[43,93] as observed in these mutants. Our data show that Kre6 is required for production of normal amounts of β-1,6-glucan and that the remaining β-1,6-glucans present in *kre6*Δ/Δ was composed of short and highly branched chains. This suggests that the Kre6 family is required for the polymerization and/or elongation of β-1,6-glucan, but not glucan branching.

In *S. cerevisiae*, only two *KRE6* family members have been identified, Kre6 and Skn1, and their absence led to strong growth defects and hypersensitivity to cell wall perturbing agents –similar to what we observed here in *C. albicans* [94]. In *C. neoformans*, among the six *KRE6* homologs, *KRE6* and *SKN1* are required for the production of cell wall β-1,6-glucan[95] and although the *KRE6* family is essential for β-1,6-glucan synthesis, its biochemical function remains unknown. Kre6 homologs are type II membrane proteins with a GH-16 domain at the luminal C-terminus and an unfolded cytosolic *N*-terminal tail[96]. Yeast Kre6 and Skn1 proteins have moderate similarity with diatom TGS (1,6-β-transglycosylase) proteins[97,98] and can synthesize glucan from UDP-Glc[99]. Kre6 homologs share structural similarities with β-glucanases and β-transglycosylases, arguing for a possible cell wall remodeling function. In *S. cerevisiae*, Kre6p has been localized in the endoplasmic reticulum, the plasma membrane and secretory vesicle-like compartments[66,96,100], and the cytosol tail was shown to be essential for the correct cellular localization and β-1,6-glucan synthesis[96]. Surprisingly, in *C. albicans* the cytosol tail is not essential[44], suggesting some functional differences of this protein in these yeasts. In *C. albicans*, the double *KRE6/SKN1* mutant is avirulent in a mice model of candidiasis[44], showing that the β-1,6-glucan biosynthetic pathway is a potential virulence target. However, the drugs Jervine (steroidal alkaloid) and a pyridobenzimidazole derivate (D75-4590), that may target Kre6 and inhibit *S. cerevisiae* growth[101,102], had no effect on *C. albicans*[101,102], presumably representing species-specific differences in drug profiles. Kre6 family members are present in all fungal pathogens producing cell wall β-1,6-glucans and further investigations are required to understand the enzyme activities and the diversity of structures related to the potential drug-targeting of these proteins.

Overall, this work highlights the central role that β-1,6-glucan plays in orchestrating cell wall synthesis during growth and in response to stress and sets the focus for further work that can exploit this central role in mitigating fungal infections.

Methods

Ethics statement

Human blood samples were taken from healthy donors from Etablissement Français du Sang Trinité (Paris, France) with written and informed consent, as per the guidelines provided by the institutional ethics committee, Institut Pasteur (convention 12/EFS/023).

Strains and growth conditions

The *Candida albicans* strains used in this study are listed in Table S1. The reference strain SC5314, used for all stress conditions, was grown overnight in 25 mL flasks, at 37°C, 180 rpm, in SD medium (2% glucose, 0.67% yeast nitrogen base with amino acids (YNB) (BD), pH 5.4). Overnight cultures were diluted to an OD_{600}= 0.001, in 50 mL fresh SD medium, incubated at 37°C, 180 rpm, and then

harvested either when reaching mid-exponential phase (OD_{600} ~ 3-5) or at stationary phase (OD_{600} ~ 11-12 after 30h). The following growth conditions were selected: hypha induction (SD containing 2% GlcNAc instead of 2% glucose, pH 7.2, no yeast-form was observed in this medium), temperature (30°C), osmolarity (1M NaCl), carbon source (SD containing 2% lactate (ChemCruz) instead of 2% glucose), oxygen limitation (hypoxia: 1% O_2, 5% CO_2, anaerobic chamber (Baker Ruskinn, I-CONIC, Bugbox M)) and oxidative stress (H_2O_2 1.5 mM, Prolabo). For studies of the effect of medium pH, SD medium was buffered with 100 mM MES (Sigma) at pH 4 or 5.4 or with MOPS (Sigma) at pH 7.5. For experiments on the effects of short-chain fatty acids (SCFAs), SD medium was supplemented with 100 mM MES and 50 mM acetate (Sigma) or 20 mM propionate (Sigma) or 15 mM butyrate (Sigma) and buffered to pH 5.4. Drugs were tested at sub-lethal concentrations: Calcofluor White (CFW, 400 µg/mL, Sigma-Aldrich), Congo Red (CR, 50 µg/mL, Sigma), tunicamycin (0.125 µg/mL, Sigma), nikkomycin (16 µg/mL, Sigma) and caspofungin (0.015 µg/mL, Sigma). Biofilm production was induced in SD medium at 37°C for 48h in 6 well plates as previously described with some modifications[103]. Overnight cultures were diluted at OD_{600}=0.2 in 6 well polystyrene plates (TPP) in 2 mL of minimal medium (SD: 2% glucose, 0.67% yeast nitrogen base without amino acids (BD), pH 5.4) supplemented by arginine 0.1 g/L, histidine 0.1g/L, uridine 0.02 g/L and methionine 0.2 g/L. The plates were incubated at 37°C, 60 min at 110 rpm for initial cell adhesion. Then, the plates were washed with 2 mL of fresh medium, and 4 mL of fresh medium was added. Plates were then sealed with Breathseal sealing membranes (Greiner Bio-one) and incubated at 37°C, 110 rpm. After 48 h, supernatant culture was aspirated, the wells were gently washed with PBS and biofilm was collected in PBS.

Cell wall mutant strains were grown at 30°C, 180 rpm, in SD medium supplemented with arginine (100 µg/mL), uridine (100 µg/mL) and histidine (20 µg/mL). The *phr1*Δ/Δ mutant was grown in SD buffered medium at pH 7.5 (with 100 mM MOPS), and the *phr2*Δ/Δ mutant at pH 5.5 (with 100 mM MES). The conditional mutant P_{MRP1}-*CHS1/chs1*Δ was first precultured in YNB with 2% maltose as a carbon source to allow the *MRP1* promoter expression and then it was grown, as all other mutants, in SD (carbon source glucose), under which condition the promoter is repressed.

Cell wall fractionation

After growth culture, the fungal biomass was collected by centrifugation (5 min, 3300 g), washed and disrupted in 200 mM Tris-HCl pH 8 using a cell disruptor (FastPrep, MPbio, 6 cycles, 6 m/s, 60 sec) with 0.3 mm glass beads (Braun). The cell wall was collected by centrifugation (5 min, 3300 g), washed twice with 200 mM Tris-HCl, pH 8, then twice with milliQ water and freeze-dried. The wall polymers were then fractionated as previously described[104]. Briefly, non-covalently bound proteins were extracted by the following treatment: dried cell wall was treated twice in 50 mM Tris-HCl, 50 mM EDTA, pH 7.5, 2% SDS, 40 mM β-mercaptoethanol in boiling water for 10 min (10-20 mg of cell

wall/mL). After centrifugation (10 min, 3300 g), three volumes of ethanol were added to the supernatant and kept overnight at +4°C. The precipitate (SDS-β-ME fraction) was collected by centrifugation (10 min, 3300 g) and dialyzed against water before freeze-drying. Other cell wall pellet was washed three times with 150 mM NaCl and extracted twice with a 1 M NaOH containing 1 mg/mL BH_4Na (Sigma), at 10-20 mg of cell wall/mL at 65°C for 1 h. After centrifugation (10 min, 3300 g), the alkali-soluble extract (AS fraction, supernatant) was neutralized with acetic acid, extensively dialyzed against water and freeze-dried. The alkali-insoluble fraction (AI fraction, pellet) was washed three times with distilled water and freeze-dried. Of note, the cell disruption was a key step to remove glycogen from cell wall extracts (Fig. S7).

Cell wall polymers quantification

Cell wall polymers of the three cell wall fractions (SDS-β-ME, AI and AS fractions) were quantified as previously described[104]. Briefly, total neutral sugars were quantified by the phenol-sulfuric acid colorimetric assay using glucose as a standard[105]. Proteins were quantified by colorimetry using the Pierce™ BCA Protein Assay Kit (ThermoScientific) according to the manufacturer's instructions. Monosaccharides, glucose and mannose, were identified and quantified by gas liquid chromatography (Perichrom) as their alditol acetates obtained after hydrolysis (4 N trifluoroacetic acid (TFA, Sigma), 100 °C, 4 h)[106]. Glucosamine was quantified by high performance anion exchange chromatography (HPAEC, Dionex, ICS-3000) on a CarboPAC-PA1 column (ThermoScientific, 250 mm x 4.6 mm) after acid hydrolysis (6 M HCl, 6 h, 100 °C) using glucosamine as a standard. Samples were eluted at a flow rate of 1 mL/min with 18 mM NaOH for 15 min, then with a linear gradient to 300 mM sodium acetate (AcONa) in 100 mM NaOH for 20 min and finally under isocratic conditions with 300 mM AcONa in 100 mM NaOH for 5 min. The column was equilibrated for 20 min with the initial buffer before injection. Samples were detected on a pulsed electrochemical detector.

Quantification of β-1,6-glucan in alkali-insoluble (AI) and alkali-soluble (AS) fractions

To quantify β-1,6-glucan in the AI fraction, a colorimetric assay was used. Oxidation with periodate allows specific degradation of vicinal carbons bearing hydroxyl groups. In the AI fraction, only β-1,6-glucans were sensitive to this treatment, leading to the formation of aldehyde functions, which were quantified in the presence of 4-hydroxybenzhydrazide (PAHBAH) (Sigma) (Fig. S8). Oxidation was carried out at 50°C for 6 h on 100 µL of AI fraction (0.5 mg/mL) with 100 µL of 25 mM *m*-IO_4Na (Sigma-Aldrich). Excess of reagent was quenched with 100 µL sodium sulfite 200 mM (Sigma). Then, 100 µL of reaction mixture were added to 900 µL of PAHBAH reagent (0.63 g sodium sulfite, 5 mL NaOH 5 M, 5 mL sodium citrate 0.5 M, 5 mL $NaCl_2$ 0.2 M qsp 100 mL milliQ water, 1 g PAHBAH) and placed in a boiling water bath for 10 min. The quantification of produced aldehyde was measured

by the absorbance at 405 nm. Pustulan (linear β-1,6-glucan, Elicityl OligoTech) was used as a standard. The β-1,3-glucan content of the AI fraction was calculated as the total glucose content after subtraction of the amount of β-1,6-glucan.

The presence of mannan in the AS fraction prevents to use the colorimetric assay of β-1,6-glucan after periodate oxidation. β-1,3-glucan and β-1,6-glucan of the AS fraction were therefore quantified by enzyme digestion. The AS fraction was digested with the endo-β-1,3-glucanase, LamA (from *Thermotoga neapolitana* expressed in *E. coli*)[107] or with an endo-β-1,6-glucanase (from *Schizosaccharomyces pombe* expressed in *Pichia pastoris*)[108]. Digestions were carried out at 37°C during 24 h by treating 0.2 mg of AS fraction with 20 µL of LamA (specific activity: 10 µmol eq/min/µL) or 60 µL of the endo-β-1,6-glucanase (specific activity: 3.03×10^{-6} µmol eq/min/µL), in 50 mM NaOAc, pH 6, in a final volume of 200 µL. Both enzymatic treatments released more than 95% of glucan. Products were quantified by the amount of released reducing sugars using the PAHBAH reagent[109] and identified by HPAEC on a CarboPAC-PA1 column (ThermoScientific). Soluble and purified β-1,6-glucans from *C. albicans* and a commercial source of laminarin (Sigma) were used as standards. Products from enzymatic digestion were eluted under the following gradient: isocratic step of 98% of eluent A (50 mM NaOH) and 2% of eluent B (500 mM AcONa in 50 mM NaOH) for 2 min, 2–15 min of a linear gradient of AcONa in 50 mM NaOH (2% B to 20% B), 15–20 min of a linear gradient (20% B to 43% B), 20–22 min of a linear gradient (43% B to 100% B), 22–25 min under isocratic conditions with 100% B. The column was equilibrated for 20 min with initial buffer before injection.

Structural characterization of β-1,6-glucan

β-1,6-glucan are branched by β-1,3 linked glucose or laminaribiose on the main chain[32,33]. Branching was estimated by enzymatic digestion by an endo-β-1,6-glucanase as previously described[33]. A 0.1 mg sample of the AI fraction was digested for 48 h at 37°C in a final volume of 100 µL with 30 µL of endo-β-1,6-glucanase in 50 mM sodium acetate, pH 6, 5 mM NaN_3. Degradation products were analysed by HPAEC on a CarboPAC-PA1 column as described above. Branching was estimated by the ratio of branched oligosaccharides on total degradation products, to which a coefficient of correction was applied. This coefficient (43.1) was calculated from a branching rate of 6.9% of purified β-1,6-glucan established by NMR (see below and table S2). Branching of β-1,3-glucan was determined in the same way after digestion of the AI fraction with LamA.

The size of the β-1,6-glucan chain was estimated by gel filtration chromatography. First, β-1,6-glucans were released by incubation at 37°C for 48 h of the AI fraction (0.5 mg) with LamA (100 µL) in 70 mM sodium acetate, pH 6, 5 mM NaN_3, in a final volume of 700 µL. After 3 min centrifugation at 12000 g, the supernatant was concentrated under vacuum (SpeedVac concentrator). Then, the sample was submitted to a gel filtration on a Superdex^{TM} 200 column (300 × 10 mm, Cytiva), eluted

with ammonium acetate 150 mM, pH 4 at a flow rate of 0.2 mL/min. Samples were detected by a refractive index detector (Iota-2, Precision Instruments). The column was calibrated with dextran molecular weight standards (6, 10, 40, 70 and 500 kDa; GE Healthcare).

Nuclear magnetic resonance (NMR)

NMR experiments were recorded at 318.15 °K using a Bruker (Billerica, USA) 800 MHz Avance NEO spectrometer with an 18.8 Tesla magnetic field equipped with a cryogenically-cooled triple resonance (^{1}H,^{13}C,^{15}N) TCI probe. Spectra were recorded using TopSpin 4.2 (Bruker) and analyzed with CCPNMR Analysis 2.5.2[110]. ^{1}H and ^{13}C chemical shifts were referenced to external DSS (2,2-dimethyl-2-silapentane-5-sulfonate, sodium salt). After three cycles of exchange (dissolution/lyophilization) against D_2O, 5 mg of purified polysaccharide were dissolved in 550 µL of D_2O (99.99% 2H, Eurisotop, Saclay, France) and placed in a 5 mm tube (Norell HT). Resonance assignment, glycosidic bonds identification and J coupling determination were achieved following standard procedures from homonuclear ^{1}H 1D, 2D COSY[111], NOESY[112] (150 ms mixing time) and natural abundance heteronuclear ^{1}H-^{13}C experiments: edited HSQC[113,114], CLIP-HSQC[115], H2BC[116], HMBC[117] and HSQC-TOCSY[114] (100 ms mixing time). The anomeric configuration of monosaccharide residues was established from the corresponding chemical shifts and $^{1}J_{H_1\text{-}C_1}$ coupling constants obtained from CLIP-HSQC spectra. Glycosidic bonds were identified using HMBC experiments and confirmed with NOESY data. $^{3}J_{H_1\text{-}H_2}$ coupling constants were measured from ^{1}H 1D spectra. The relative amount of monosaccharide residues was estimated from the integrals on ^{1}H 1D spectra obtained at 333.15 °K using a total recovery delay of 12 s.

Transmission electron microscopy

Cells were grown as described above and volumes of culture media equivalent to a quantity of cells equivalent to OD_{600nm}=1 were collected and centrifuged 5 min at 3300 g. Cells were chemically fixed at room temperature in the dark for 1 h with 2.5% glutaraldehyde (Sigma) in fresh culture media (10 mL), washed in 1X PHEM buffer (60 mM PIPES, 25 mM HEPES, 10 mM EGTA, 2 mM $MgCl_2$, pH 7.3) and centrifugated at low speed. The pellets were then resuspended in a droplet of 1X PHEM buffer and taken up into cellulose capillary tubes. For each strain, the capillaries were cut into 3 mm pieces, placed in 6 mm type A specimen carrier (side 0.2 mm) filled with hexadecen, covered by 6 mm type B carrier (side flat) and frozen with a high-pressure freezing machine (EM ICE, Leica microsystems) as previously described[118]. The samples were then freeze-substituted in a mix of 1% OsO4, 5% H_2O in pure acetone for 24 h at -90°C, 12 h at 5°C/h at -30°C, 12 h at -30°C, 3 h at 10°C/h until 0°C and 1 h at 0°C. All samples were washed in pure acetone, and gradually infiltrated under agitation in low viscosity Spurr resin/acetone mix from 30% to 100%, as previously described[119]. Samples were then embedded in pure Spurr resin (EMS), followed by polymerization for 48 h at

60°C. Ultrathin sections (70 nm) were cut with a Leica Ultracut S microtome, and stained with 4% uranyl acetate and then 3% lead citrate. Transmission electron microscopy (TEM) images were captured with a Tecnai Spirit 120 kV TEM equipped with a bottom-mounted Eagle 4kx4k camera (FEI, USA). For statistical analysis, internal and external cell wall thickness have been measured (between 37-40 measurements, on 7-13 cells per condition) using TEM Imaging and Analysis software (TIA, FEI, USA).

Immunolabeling

Rabbit polyclonal antibodies were produced by ProteoGenix (Schiltigheim, France) using pustulan-conjugated BSA as the antigen. After 7-8 weeks of immunization, the resulting serum was used without antibodies purification. The specificity of serum was tested on pustulan, curdlan and cell wall AI fractions from *Aspergillus fumigatus* (which did not contain β-1,6-glucan) and *C. albicans* by ELISA (not shown). For immunolabelling of β-1,6-glucans and β-1,3-glucans in the cell wall of *C. albicans*, cells were grown as described above. Then, 1 mL of culture was fixed at ambient temperature in the dark (1-2 h) with paraformaldehyde 3.8% (PFA, Electron Microscopy Sciences). Cells were then centrifuged 3 min at 8000 g and washed 3 times with 500 µL PBS. In each step, cells were resuspended vigorously to separate the cells and disperse aggregates. Then, cells were resuspended vigorously in 500 µL of PBS and 5% goat serum (Sigma) and then 20 µL were added to each well of a slide (Diagnostic Microscope Slides, 8 well 6 mm, ThermoScientific) coated poly-L-lysine 0.1% and incubated 1 h at ambient temperature to permit cell adhesion. Liquid was removed and PBS 1X and 5% goat serum was added again and incubated during 1 h at ambient temperature. The liquid was aspirated and 20 µL of first antibody was added in PBS 1X and 5% goat serum overnight at 4°C (dilution 1/100 for polyclonal anti-β-1,6-glucan produced in rabbit, 1/250 for monoclonal anti-β-1,3-glucan (named 5H5) produced in mouse and kindly provided by N. Nifantiev[120]). Wells were washed three times with PBS 1X and 5% goat serum. The second antibody was then added in PBS 1X and 5% goat serum 1h at ambient temperature (dilution 1/200, Alexa Fluor™ 488 goat anti-mouse IgG (AF488, molecular probes) or fluorescein goat anti-rabbit IgG (FITC, Invitrogen)). Wells were washed 3 times with PBS and 5% (v/v) goat serum and once with PBS. Then, one drop of Fluoromount-G (Invitrogen) was added to each well, wells were covered with a coverslip N°1.5 (Menzel-Gläser), and polymerization was done during 48 h. Cells were observed on an EVOS FL microscope (Life Technologies), with a magnification x100 objective with oil immersion.

PBMC and neutrophil isolation, stimulation by parietal fractions and cytokine quantification

Human peripheral blood mononuclear cells (PBMCs) from heathy donors were isolated by a density-gradient separation of Ficoll 400 (Eurobio, France). Isolated PBMCs were re-suspended in RPMI

1640 + GlutaMAX™ medium (Gibco), supplemented by 20% normal human sera (NHS, Normal Human Serum-Pooled, Zenbio) and seeded in each well (100 µL containing $4x10^6$ cells/mL) of 96-well microtiter plates (TPP). Cell wall fractions suspended in RPMI 1640 + GlutaMAX™ medium were then added, at a final concentration of 25 µg/mL. LPS (Sigma, 0.1 µg/mL) was used as a positive control. After 24 h incubation at 37°C in a 5% CO_2 chamber (Cytoperm 2, ThermoFisher Scientific), the culture supernatants were collected and stored at -20°C until further analysis.

Neutrophils from healthy donors were isolated with EasySep™ Direct Human Neutrophil Isolation Kit (STEMCELL Technologies) according to manufacturer's instructions. Isolated neutrophils were re-suspended in RPMI 1640 + GlutaMAX™ medium (Gibco) and seeded in each well (100 µL containing $1x10^6$ cells/mL) of 24-well microtiter plates (TPP). 200 µL of NHS at 3% diluted in RPMI 1640 + GlutaMAX™ medium were the added. Cell wall fractions suspended in RPMI 1640 + GlutaMAX™ medium were then added, at a final concentration of 25 µg/mL. LPS (0.1 µg/mL) was used as a positive control. After 16 h incubation at 37°C in a 5% CO_2 chamber (Cytoperm 2, ThermoFisher Scientific), the culture supernatants were collected and stored at -20°C until further analysis.

Global cytokines, chemokines, and acute phase proteins (total 36) present in the supernatants were detected with using Proteome Profiler Human Cytokines Array Kit (R&D Systems) according to manufacturer's instructions. Following, the cytokines, chemokines and acute phase proteins of interest identified through protein profiler were quantified using DuoSet ELISA kits (R&D Systems) according to the manufacturer's instructions.

Native AI and periodate oxidized AI (AI-OxP) fractions and purified β-1,6-glucans from *C. albicans* were used. AI-OxP fraction was generated by the treatment of 40 mg of AI fraction with 100 mM *m*-IO_4Na (4 mL), 3 days at 4°C. The reaction was stopped by addition of 200 µL of glycerol, oxidized fraction was washed by centrifugation with water, reduced with BH_4Na (10 mg/mL in 0.1 mM NaOH, overnight) then submitted to mild acid hydrolysis (AcOH 10% 100°C, 1 h) and finally washed with water and freeze-dried. Purified β-1,6-glucans were produced by digesting the AI fraction (40 mg) with LamA as described above. LamA was removed by passing the sample through a C-18 SPE cartridge (Sep-Pak classic, Waters) eluted with 5% acetonitrile and 0.1% TFA. Then, samples were purified by gel filtration chromatography (Superdex 200, 60 cm x 16 cm, Cytiva) in ammonium acetate 150 mM, pH 4 at a flow rate of 0.5 mL/min. Samples were detected by a refractive index detector (Iota2, Precision Instruments) and dialyzed against water and then freeze-dried. The fractions were quantified by the phenol-sulfuric acid colorimetric assay as previously described.

Complement activation

Complement activation was done as previously described[121]. Briefly, cell wall fraction from *C. albicans*: AI, AI-OxP and purified β-1,6-glucans were coated on 96-well microtiter plates (100 µL/well) at three different concentrations 50 µg, 25 µg and 12.5 µg per well in 50 mM bicarbonate buffer, pH 9.6, overnight at ambient temperature. Then, supernatants were discarded, and wells were blocked with PBS 1X/BSA 1% for 1h at ambient temperature. Then 8 µL of NHS and 92 µL of Gelatin veronal buffer (GVB, 5 mM barbital, 145 mM NaCl, 0.1% gelatin, pH 7.4) supplemented by $MgCl_2$ (0.5 mM) and $CaCl_2$ (0.15 mM) were added, incubated for 1 h, and then washed three times with PBS 1X/Tween-20 0.05%. Complement activation was measured by quantifying deposited C3b upon adding the wells with mouse monoclonal anti-human C3b antibody (MA1-82814, ThermoFisher Scientific, diluted 1:1,000) diluted in PBS 1X/BSA 1% and incubating 1 h at ambient temperature, washing the wells with PBS 1X/Tween 20 0.05%, adding the wells with peroxidase-conjugated secondary anti-mouse IgG antibodies (Sigma-Aldrich, diluted 1:1,000) and incubating for 1h at ambient temperature. After washing, 100 µL of substrate solution (TMB, BioFX; 100 µL/well) was added and the reaction was stopped with 50 µL of 4% H_2SO_4. The absorbance was read at 450 nm after subtraction of reference wavelength at 540 nm using microplate reader (Infinite m200 pro, TECAN).

Generation of mutants by transient CRISPR/Cas9

Homozygous null mutants (*kre6*Δ/Δ*;* *skn1*Δ/Δ; *kre62*Δ/Δ *;* *skn2*Δ/Δ *;* *kre6/skn1*Δ/Δ*;* *kre6/skn1/kre62/skn2*Δ/Δ*)* were generated in *C. albicans* SC5314 using established transient CRISPR-Cas9 methods[122,123]. A sgRNA cassette was constructed by PCR, first by synthesising the SNR52 promoter (using primers SNR52/F and SNR52/R/GOI) and the sgRNA scaffold (with the primers sgRNA/F/GOI and sgRNA/R), using plasmid pV1093 as a template[122]. These two products were fused by PCR, followed by nested PCR with primers SNR52/N and sgRNA/N. The *CaCAS9* cassette was amplified from the plasmid pV1093 with primers CaCas9/F and CaCas9/R. Repair templates (RT), which contained the *SAT1*-Flipper marker and harboured 80 bp homology to the 5' and 3' ends of the target gene, were amplified from pSFS2A[124]. The RT containing the hygromycin resistance gene *HygB* was amplified from pCrispr-gRNA1/hygR, derived from plasmid pV1090[122] as follows: a *BspHI* fragment carrying the *HygB* marker was cut from pYM70[125], the ends filled in with the Klenow enzyme and the fragment ligated into pV1090 digested with *StuI* and *BglII* and treated with the Klenow enzyme. PCR reactions to amplify sgRNA and CaCas9 were carried out using Phusion High-Fidelity DNA polymerase (NEB), and Q5 polymerase (NEB) was used for RT amplification, according to the manufacturer's instructions. All PCR products were cleaned-up and concentrated with NucleoSpin Gel and PCR Clean-up (Macherey-Nagel). PCR products (3 µg of CaCAS9 cassette, 1 µg of sgRNA cassette and 3 µg of the relevant RT) were transformed into *C.*

albicans SC5314 using the lithium acetate method[126]. Transformants were selected on YPD containing 150 µg/mL nourseothricin (Jena Bioscience) or YPD with 600 µg/mL hygromycin (Sigma). Disruption of both alleles of the target locus and integration of the RT were confirmed by PCR after DNA extraction (MasterPure Yeast DNA Purification Kit, Lucigen). The *SAT1* gene was removed with the flipper system. Briefly, the transformants were cultivated overnight in 3 mL YP with 2% maltose at 30°C. Then, the culture was diluted to 250 cells/mL in sterile water and 200 µL were plated on YPD with 25 µg/mL nourseothricin and incubated 1-2 days at 30°C. The smaller colonies were replicated on YPD vs. YPD + 150 µg/mL nourseothricin. Transformants that grew only YPD were checked by PCR using primers Flanking_F/GOI and Flanking_R/GOI. The primers used for the construction and PCR check of these mutants are described in Table S3. Deletions were validated by PCR (Fig. S9).

The quadruple mutant *kre6/skn1/kre62/skn2*Δ/Δ was complemented by integrating a StuI-linearized plasmid bearing the *KRE6* gene under the control of the constitutive promoter *ACT1* at the *RPS1* locus. This plasmid was obtained using the Gateway™ technology (Invitrogen™) as described previously[127]. *KRE6* was PCR amplified on SC5314 genomic DNA with primers KRE6-FWD and KRE6-REV; the fragment was cloned in pDONR207[128] with the Invitrogen™ Gateway BP clonase, and then transferred to the destination vector CIp10-P$_{ACT1}$-*SAT1*[129] using the Invitrogen™ Gateway LR clonase. Successful cloning into the destination vector was confirmed by sequencing. Transformants were selected on YPD+100 µg/mL nourseothricin. Plasmid integration at the *RPS1* locus was checked by colony PCR using CIpUL and CIpSAT.

Phenotypic analyses

Kinetic curves were generated in 96 well plate (TPP) in SD medium, 30°C, at initial $OD_{620\ nm}$= 0.01 using a Tecan Sunrise absorbance microplate reader. Optical density was measured every 10 min during 80 h with Magellan™ Software. Doubling time was calculated from growth curves with GraphPad Prism software by generating a nonlinear regression (logistic curve) to determine the *k* coefficient, and then calculated as doubling time = ln(2)/k.

Spot test drug sensitivity assays were performed on complete SD medium agar plates containing either Congo Red (50 µg/mL), Calcofluor White (50 µg/mL), tunicamycin (1 µg/mL), nikkomycin (32 µg/mL) or caspofungin (0.5 µg/mL). Cell were precultured for 24 h in SD medium liquid, 30°C, and then diluted to $OD_{600\ nm}$=1 in sterile water, and then 10-fold serially diluted. Samples of 5 µL of each concentration were spotted onto agar plates. Pictures of plates were taken after 24 h, 48 h, 72 h and 6 days with a Phenobooth+ Colony counter (Singer Instruments). To observe macroscopic filamentation, 5 µL ($OD_{600\ nm}$=1) were spotted on YNB 2%GlcNAc, buffered at pH 7.2 with 100 mM MOPS agar, at 37°C, for 6 days. Pictures were taken using an I-phone camera.

To observe hyphal growth, cells were grown overnight in SD liquid 30°C, then diluted to $OD_{600\ nm}$=0.2 in 1 mL of 24 well plate (TPP) and growth for 6 h either in SD, 30°C (control, no-filamentation) or in YNB 2%GlcNAc, buffed at pH 7.2 with 100 mM MOPS, at 37°C (inducing filamentation). Cells were then observed with an Olympus IX 83 microscope and images were captured with a Hamamatsu ORCA Flash cooled CCD camera, using the cellSens imaging software.

Statistical analyses

GraphPad Prism 10 software was used for statistical analyses. Data were generated from at least three independent biological replicates and then expressed as means ± standard deviation. Specific tests are indicated in the figure legends. Normally distributed datasets (QQ plot or Shapiro-Wilk test), were compared with ordinary one-way ANOVA (Dunnett's or Tukey's multiple comparisons test) or two-tailed unpaired *t*-test. For immunology data, measurements were paired/dependant as the same donors were exposed to different cell wall fractions, thus we applied the nonparametric test for non-normally distributed data: Friedman test (with Dunn's multiple comparisons test). P-values (P) < 0.05 were considered as significant and represented on graphs as followed: *, P < 0,05 ; **, P < 0,01 ; ***, P < 0,001 ; ****, P < 0,0001 ; ns : non-significant.

Acknowledgements

C.B is the recipient of a Ph.D. fellowship from the Laboratoire d'Excellence Integrative Biology of Emerging Infectious Diseases (ANR-10-LABX-62-IBEID). We acknowledge support from the French Government's Investissement d'Avenir program (Laboratoire d'Excellence Integrative Biology of Emerging Infectious Diseases [ANR-10-LABX-62-IBEID]) and Institut Pasteur from Paris. V.A. and T.F. are supported by the Agence Nationale de la Recherche ANR-21-CE17-0032-01, FUNPOLYVAC grant. We thank Romain Laurian and Natacha Sertour for their advice for molecular biology, Cécile Gautier for her advice on Prism software and spotting assays, Catherine Comte, Lucia Oreus and Jamal Boutchlhit for material availability and Matt Edmondson for providing *C. albicans* strains. The authors thanks Suzan Noble, Mathias Richard and Neil Gow for the access to their deletion mutant collections. NG acknowledges support of Wellcome Trust Investigator, Collaborative, Equipment, Strategic and Biomedical Resource awards (101873, 200208, 215599, 224323). NG also thanks the MRC (MR/M026663/2) and the MRC Centre for Medical Mycology (MR/N006364/2) for support. This study/research is funded by the National Institute for Health and Care Research (NIHR) Exeter Biomedical Research Centre (BRC). The views expressed are those of the author(s) and not necessarily those of the NIHR or the Department of Health and Social Care. The 800-MHz NMR spectrometer of the Institut Pasteur was partially funded by the Région Ile de France (SESAME 2014 NMRCHR grant no 4014526). CS is grateful for support for equipment from

the French Government Programme Investissements d'Avenir France BioImaging (FBI, N° ANR-10-INSB-04-01).

Author contributions

C.B., V.A., S.B.B, N.G. and T.F. designed experiments and analyzed data. C.B. performed most of the experiments. I.V. and M.C. constructed strains. C.S. and T.M. designed and performed electron microscopy experiments. I.G. performed NMR experiments and analysis. NG provided essential strains and materials. C.B., V.A., C.dE., N.G. and T.F wrote the manuscript. All authors have read and agreed to the published version of the manuscript.

Competing interests

The authors declare no competing interests.

References

1. Denning, D. W. Global incidence and mortality of severe fungal disease. *Lancet Infect. Dis.* S1473-3099(23)00692–8 (2024) doi:10.1016/S1473-3099(23)00692-8.

2. Brown, G. D. *et al.* Hidden Killers: Human Fungal Infections. *Sci. Transl. Med.* 4, 165rv13-165rv13 (2012).

3. Sharma, M. & Chakrabarti, A. Candidiasis and Other Emerging Yeasts. *Curr. Fungal Infect. Rep.* 17, 15–24 (2023).

4. d'Enfert, C. *et al.* The impact of the Fungus-Host-Microbiota interplay upon *Candida albicans* infections: current knowledge and new perspectives. *FEMS Microbiol. Rev.* 45, fuaa060 (2021).

5. WHO fungal priority pathogens list to guide research, development and public health action. https://www.who.int/publications-detail-redirect/9789240060241.

6. Hall, R. A. Dressed to impress: impact of environmental adaptation on the *Candida albicans* cell wall. *Mol. Microbiol.* 97, 7–17 (2015).

7. Mishra, R., Minc, N. & Peter, M. Cells under pressure: how yeast cells respond to mechanical forces. *Trends Microbiol.* 30, 495–510 (2022).

8. Brown, G. D. Innate antifungal immunity: the key role of phagocytes. *Annu. Rev. Immunol.* 29, 1–21 (2011).

9. Netea, M. G., Joosten, L. A. B., van der Meer, J. W. M., Kullberg, B.-J. & van de Veerdonk, F. L. Immune defence against *Candida* fungal infections. *Nat. Rev. Immunol.* 15, 630–642 (2015).

10. Netea, M. G. Immune sensing of *Candida albicans* requires cooperative recognition of mannans and glucans by lectin and Toll-like receptors. *J. Clin. Invest.* 116, 1642–1650 (2006).

11. Erwig, L. P. & Gow, N. A. R. Interactions of fungal pathogens with phagocytes. *Nat. Rev. Microbiol.* 14, 163–176 (2016).

12. Dambuza, I. M., Levitz, S. M., Netea, M. G. & Brown, G. D. Fungal Recognition and Host Defense Mechanisms. *Microbiol. Spectr.* 5, (2017).

13. Lionakis, M. S. & Levitz, S. M. Host Control of Fungal Infections: Lessons from Basic Studies and Human Cohorts. *Annu. Rev. Immunol.* 36, 157–191 (2018).

14. Urban, C. F., Reichard, U., Brinkmann, V. & Zychlinsky, A. Neutrophil extracellular traps capture and kill *Candida albicans* yeast and hyphal forms. *Cell. Microbiol.* 8, 668–676 (2006).

15. Gow, N. A. R., van de Veerdonk, F. L., Brown, A. J. P. & Netea, M. G. *Candida albicans* morphogenesis and host defence: discriminating invasion from colonization. *Nat. Rev. Microbiol.* 10, 112–122 (2011).

16. Gow, N. A. R. & Hube, B. Importance of the *Candida albicans* cell wall during commensalism and infection. *Curr. Opin. Microbiol.* 15, 406–412 (2012).

17. Brown, G. D. *et al.* Dectin-1 is a major beta-glucan receptor on macrophages. *J. Exp. Med.* 196, 407–412 (2002).

18. Brown, G. D. & Gordon, S. Fungal beta-glucans and mammalian immunity. *Immunity* 19, 311–315 (2003).

19. Taylor, P. R. *et al.* Dectin-1 is required for beta-glucan recognition and control of fungal infection. *Nat. Immunol.* 8, 31–38 (2007).

20. Ferwerda, B. *et al.* Human dectin-1 deficiency and mucocutaneous fungal infections. *N. Engl. J. Med.* 361, 1760–1767 (2009).

21. Marakalala, M. J. *et al.* Differential adaptation of *Candida albicans in vivo* modulates immune recognition by dectin-1. *PLoS Pathog.* 9, e1003315 (2013).

22. Wagener, J. *et al.* Fungal chitin dampens inflammation through IL-10 induction mediated by NOD2 and TLR9 activation. *PLoS Pathog.* 10, e1004050 (2014).

23. Hall, R. A. & Gow, N. A. R. Mannosylation in *Candida albicans*: role in cell wall function and immune recognition. *Mol. Microbiol.* 90, 1147–1161 (2013).

24. Choudhury, Q. J. *et al.* Dectin-3-targeted antifungal liposomes efficiently bind and kill diverse fungal pathogens. *Mol. Microbiol.* 120, 723–739 (2023).

25. Sem, X. *et al.* β-glucan Exposure on the Fungal Cell Wall Tightly Correlates with Competitive Fitness of *Candida* Species in the Mouse Gastrointestinal Tract. *Front. Cell. Infect. Microbiol.* 6, (2016).

26. Hopke, A., Brown, A. J. P., Hall, R. A. & Wheeler, R. T. Dynamic Fungal Cell Wall Architecture in Stress Adaptation and Immune Evasion. *Trends Microbiol.* 26, 284–295 (2018).

27. Lenardon, M. D., Sood, P., Dorfmueller, H. C., Brown, A. J. P. & Gow, N. A. R. Scalar nanostructure of the *Candida albicans* cell wall; a molecular, cellular and ultrastructural analysis and interpretation. *Cell Surf. Amst. Neth.* 6, 100047 (2020).

28. Graus, M. S. *et al.* Mannan Molecular Substructures Control Nanoscale Glucan Exposure in *Candida*. *Cell Rep.* 24, 2432-2442.e5 (2018).

29. Gow, N. A. R., Latge, J.-P. & Munro, C. A. The Fungal Cell Wall: Structure, Biosynthesis, and Function. *Microbiol. Spectr.* 5, (2017).

30. Klis, F. M., Sosinska, G. J., de Groot, P. W. J. & Brul, S. Covalently linked cell wall proteins of *Candida albicans* and their role in fitness and virulence. *FEMS Yeast Res.* 9, 1013–1028 (2009).

31. Liu, W. *et al.* Bst1 is required for *Candida albicans* infecting host via facilitating cell wall anchorage of Glycosylphosphatidyl inositol anchored proteins. *Sci. Rep.* 6, 34854 (2016).

32. Iorio, E. *et al. Candida albicans* cell wall comprises a branched β-d-(1→6)-glucan with β-d-(1→3)-side chains. *Carbohydr. Res.* 343, 1050–1061 (2008).

33. Aimanianda, V. *et al.* Cell wall beta-(1,6)-glucan of *Saccharomyces cerevisiae*: structural characterization and in situ synthesis. *J. Biol. Chem.* 284, 13401–13412 (2009).

34. Mio, T. *et al.* Isolation of the *Candida albicans* homologs of *Saccharomyces cerevisiae* KRE6 and SKN1: expression and physiological function. *J. Bacteriol.* 179, 2363–2372 (1997).

35. Herrero, A. B. *et al. KRE5* Gene Null Mutant Strains of *Candida albicans* Are Avirulent and Have Altered Cell Wall Composition and Hypha Formation Properties. *Eukaryot. Cell* 3, 1423–1432 (2004).

36. Free, S. J. Fungal Cell Wall Organization and Biosynthesis. in *Advances in Genetics* vol. 81 33–82 (Elsevier, 2013).

37. Schiavone, M. *et al.* A combined chemical and enzymatic method to determine quantitatively the polysaccharide components in the cell wall of yeasts. *FEMS Yeast Res.* 14, 933–947 (2014).

38. Brown, J. L., Kossaczka, Z., Jiang, B. & Bussey, H. A mutational analysis of killer toxin resistance in *Saccharomyces cerevisiae* identifies new genes involved in cell wall (1-->6)-beta-glucan synthesis. *Genetics* 133, 837–849 (1993).

39. CAZy - GT24. http://www.cazy.org/GT24.html.

40. Levinson, J. N., Shahinian, S., Sdicu, A.-M., Tessier, D. C. & Bussey, H. Functional, comparative and cell biological analysis of *Saccharomyces cerevisiae* Kre5p. *Yeast* 19, 1243–1259 (2002).

41. Lesage, G. & Bussey, H. Cell wall assembly in *Saccharomyces cerevisiae*. *Microbiol. Mol. Biol. Rev. MMBR* 70, 317–343 (2006).

42. Montijn, R. C. *et al.* Localization of synthesis of beta1,6-glucan in *Saccharomyces cerevisiae*. *J. Bacteriol.* 181, 7414–7420 (1999).

43. Han, Q., Wang, N., Pan, C., Wang, Y. & Sang, J. Elevation of cell wall chitin via Ca2+ - calcineurin-mediated PKC signaling pathway maintains the viability of *Candida albicans* in the absence of β-1,6-glucan synthesis. *Mol. Microbiol.* 112, 960–972 (2019).

44. Han, Q. *et al.* Blocking β-1,6-glucan synthesis by deleting KRE6 and SKN1 attenuates the virulence of *Candida albicans*. *Mol. Microbiol.* 111, 604–620 (2019).

45. *Candida* Genome Database. http://www.candidagenome.org/.

46. Chaffin, W. L., López-Ribot, J. L., Casanova, M., Gozalbo, D. & Martínez, J. P. Cell wall and secreted proteins of *Candida albicans*: identification, function, and expression. *Microbiol. Mol. Biol. Rev. MMBR* 62, 130–180 (1998).

47. Garcia-Rubio, R., de Oliveira, H. C., Rivera, J. & Trevijano-Contador, N. The Fungal Cell Wall: *Candida, Cryptococcus,* and *Aspergillus* Species. *Front. Microbiol.* 10, 2993 (2020).

48. Ruiz-Herrera, J., Elorza, M. V., Valentín, E. & Sentandreu, R. Molecular organization of the cell wall of *Candida albicans* and its relation to pathogenicity. *FEMS Yeast Res.* 6, 14–29 (2006).

49. Kollár, R. *et al.* Architecture of the yeast cell wall. Beta(1-->6)-glucan interconnects mannoprotein, beta(1-->)3-glucan, and chitin. *J. Biol. Chem.* 272, 17762–17775 (1997).

50. Braun, P. C. & Calderone, R. A. Chitin synthesis in *Candida albicans*: comparison of yeast and hyphal forms. *J. Bacteriol.* 133, 1472–1477 (1978).

51. Ene, I. V. *et al.* Host carbon sources modulate cell wall architecture, drug resistance and virulence in a fungal pathogen. *Cell. Microbiol.* 14, 1319–1335 (2012).

52. Chapman, T., Kinsman, O. & Houston, J. Chitin biosynthesis in *Candida albicans* grown *in vitro* and *in vivo* and its inhibition by nikkomycin Z. *Antimicrob. Agents Chemother.* 36, 1909–1914 (1992).

53. Roncero, C. & Durán, A. Effect of Calcofluor white and Congo red on fungal cell wall morphogenesis: *in vivo* activation of chitin polymerization. *J. Bacteriol.* 163, 1180–1185 (1985).

54. Walker, L. A., Gow, N. A. R. & Munro, C. A. Elevated chitin content reduces the susceptibility of *Candida* species to caspofungin. *Antimicrob. Agents Chemother.* 57, 146–154 (2013).

55. Gow, N. A. *et al.* A hyphal-specific chitin synthase gene (CHS2) is not essential for growth, dimorphism, or virulence of *Candida albicans*. *Proc. Natl. Acad. Sci. U. S. A.* 91, 6216–6220 (1994).

56. Preechasuth, K. *et al.* Cell wall protection by the *Candida albicans* class I chitin synthases. *Fungal Genet. Biol. FG B* 82, 264–276 (2015).

57. Munro, C. A., Schofield, D. A., Gooday, G. W. & Gow, N. a. R. Regulation of chitin synthesis during dimorphic growth of *Candida albicans*. *Microbiol. Read. Engl.* 144 (Pt 2), 391–401 (1998).

58. Mio, T. *et al.* Role of three chitin synthase genes in the growth of *Candida albicans*. *J. Bacteriol.* 178, 2416–2419 (1996).

59. Suwunnakorn, S., Wakabayashi, H., Kordalewska, M., Perlin, D. S. & Rustchenko, E. FKS2 and FKS3 Genes of Opportunistic Human Pathogen *Candida albicans* Influence Echinocandin Susceptibility. *Antimicrob. Agents Chemother.* 62, e02299-17 (2018).

60. Lee, K. K. *et al.* Yeast species-specific, differential inhibition of β-1,3-glucan synthesis by poacic acid and caspofungin. *Cell Surf.* 3, 12–25 (2018).

61. Fonzi, W. A. PHR1 and PHR2 of *Candida albicans* Encode Putative Glycosidases Required for Proper Cross-Linking of beta-1,3- and beta-1,6-Glucans. *J BACTERIOL* 181, 10 (1999).

62. Aimanianda, V. *et al.* The Dual Activity Responsible for the Elongation and Branching of β-(1,3)-Glucan in the Fungal Cell Wall. *mBio* 8, e00619-17 (2017).

63. De Bernardis, F., Mühlschlegel, F. A., Cassone, A. & Fonzi, W. A. The pH of the Host Niche Controls Gene Expression in and Virulence of *Candida albicans*. *Infect. Immun.* 66, 3317–3325 (1998).

64. Gow, N. A. R. & Lenardon, M. D. Architecture of the dynamic fungal cell wall. *Nat. Rev. Microbiol.* 21, 248–259 (2023).

65. Munro, C. A. *et al.* Mnt1p and Mnt2p of *Candida albicans* Are Partially Redundant α-1,2-Mannosyltransferases That Participate in O-Linked Mannosylation and Are Required for Adhesion and Virulence. *J. Biol. Chem.* 280, 1051–1060 (2005).

66. Shahinian, S. & Bussey, H. beta-1,6-Glucan synthesis in *Saccharomyces cerevisiae*. *Mol. Microbiol.* 35, 477–489 (2000).

67. Aebi, M., Bernasconi, R., Clerc, S. & Molinari, M. N-glycan structures: recognition and processing in the ER. *Trends Biochem. Sci.* 35, 74–82 (2010).

68. Breinig, F., Tipper, D. J. & Schmitt, M. J. Kre1p, the plasma membrane receptor for the yeast K1 viral toxin. *Cell* 108, 395–405 (2002).

69. Breinig, F., Schleinkofer, K. & Schmitt, M. J. Yeast Kre1p is GPI-anchored and involved in both cell wall assembly and architecture. *Microbiol. Read. Engl.* 150, 3209–3218 (2004).

70. CAZy - GH16. http://www.cazy.org/GH16.html.

71. Stalhberger, T. *et al.* Chemical organization of the cell wall polysaccharide core of *Malassezia restricta*. *J. Biol. Chem.* 289, 12647–12656 (2014).

72. Kottom, T. J., Hebrink, D. M., Jenson, P. E., Gudmundsson, G. & Limper, A. H. Evidence for Proinflammatory β-1,6 Glucans in the *Pneumocystis carinii* Cell Wall. *Infect. Immun.* 83, 2816–2826 (2015).

73. Ballou, E. R. *et al.* Lactate signalling regulates fungal β-glucan masking and immune evasion. *Nat. Microbiol.* 2, 16238 (2016).

74. Gow, N. A. R., Casadevall, A. & Fang, W. Top five unanswered questions in fungal cell surface research. *Cell Surf. Amst. Neth.* 10, 100114 (2023).

75. de Assis, L. J. *et al.* Nature of β-1,3-Glucan-Exposing Features on *Candida albicans* Cell Wall and Their Modulation. *mBio* 13, e02605-22.

76. Chen, T., Wagner, A. S. & Reynolds, T. B. When Is It Appropriate to Take Off the Mask? Signaling Pathways That Regulate ß(1,3)-Glucan Exposure in *Candida albicans*. *Front. Fungal Biol.* 3, 842501 (2022).

77. Rubin-Bejerano, I., Abeijon, C., Magnelli, P., Grisafi, P. & Fink, G. R. Phagocytosis by human neutrophils is stimulated by a unique fungal cell wall component. *Cell Host Microbe* 2, 55–67 (2007).

78. Palma, A. S. *et al.* Ligands for the beta-glucan receptor, Dectin-1, assigned using 'designer' microarrays of oligosaccharide probes (neoglycolipids) generated from glucan polysaccharides. *J. Biol. Chem.* 281, 5771–5779 (2006).

79. Goodridge, H. S. *et al.* Activation of the innate immune receptor Dectin-1 upon formation of a 'phagocytic synapse'. *Nature* 472, 471–475 (2011).

80. Childers, D. S. *et al.* Epitope Shaving Promotes Fungal Immune Evasion. *mBio* 11, e00984-20 (2020).

81. Yang, M. *et al.* Control of β-glucan exposure by the endo-1,3-glucanase Eng1 in *Candida albicans* modulates virulence. *PLoS Pathog.* 18, e1010192 (2022).

82. Cabib, E. Two novel techniques for determination of polysaccharide cross-links show that Crh1p and Crh2p attach chitin to both beta(1-6)- and beta(1-3)glucan in the *Saccharomyces cerevisiae* cell wall. *Eukaryot. Cell* 8, 1626–1636 (2009).

83. Cabib, E. & Durán, A. Synthase III-dependent chitin is bound to different acceptors depending on location on the cell wall of budding yeast. *J. Biol. Chem.* 280, 9170–9179 (2005).

84. Cabib, E., Blanco, N., Grau, C., Rodríguez-Peña, J. M. & Arroyo, J. Crh1p and Crh2p are required for the cross-linking of chitin to beta(1-6)glucan in the *Saccharomyces cerevisiae* cell wall. *Mol. Microbiol.* 63, 921–935 (2007).

85. Terashima, H., Yabuki, N., Arisawa, M., Hamada, K. & Kitada, K. Up-regulation of genes encoding glycosylphosphatidylinositol (GPI)-attached proteins in response to cell wall damage caused by disruption of FKS1 in *Saccharomyces cerevisiae*. *Mol. Gen. Genet. MGG* 264, 64–74 (2000).

86. Cabib, E. Two novel techniques for determination of polysaccharide cross-links show that Crh1p and Crh2p attach chitin to both beta(1-6)- and beta(1-3)glucan in the *Saccharomyces cerevisiae* cell wall. *Eukaryot. Cell* 8, 1626–1636 (2009).

87. Munro, C. A. *et al.* Chs1 of *Candida albicans* is an essential chitin synthase required for synthesis of the septum and for cell integrity. *Mol. Microbiol.* 39, 1414–1426 (2001).

88. Southard, S. B., Specht, C. A., Mishra, C., Chen-Weiner, J. & Robbins, P. W. Molecular Analysis of the *Candida albicans* Homolog of *Saccharomyces cerevisiae* MNN9, Required for Glycosylation of Cell Wall Mannoproteins. *J. Bacteriol.* 181, 7439 (1999).

89. Yadav, B. *et al.* Differences in fungal immune recognition by monocytes and macrophages: N-mannan can be a shield or activator of immune recognition. *Cell Surf. Amst. Neth.* 6, 100042 (2020).

90. Pagé, N. *et al.* A *Saccharomyces cerevisiae* genome-wide mutant screen for altered sensitivity to K1 killer toxin. *Genetics* 163, 875–894 (2003).

91. Childers, D. S. *et al.* Impact of the Environment upon the *Candida albicans* Cell Wall and Resultant Effects upon Immune Surveillance. *Curr. Top. Microbiol. Immunol.* 425, 297–330 (2020).

92. Vink, E. *et al.* An *in vitro* assay for (1 --> 6)-beta-D-glucan synthesis in *Saccharomyces cerevisiae*. *Yeast Chichester Engl.* 21, 1121–1131 (2004).

93. Rueda, C., Cuenca-Estrella, M. & Zaragoza, O. Paradoxical growth of *Candida albicans* in the presence of caspofungin is associated with multiple cell wall rearrangements and decreased virulence. *Antimicrob. Agents Chemother.* 58, 1071–1083 (2014).

94. Roemer, T., Delaney, S. & Bussey, H. SKN1 and KRE6 define a pair of functional homologs encoding putative membrane proteins involved in beta-glucan synthesis. *Mol. Cell. Biol.* 13, 4039–4048 (1993).

95. Gilbert, N. M. *et al.* KRE genes are required for beta-1,6-glucan synthesis, maintenance of capsule architecture and cell wall protein anchoring in *Cryptococcus neoformans*. *Mol. Microbiol.* 76, 517–534 (2010).

96. Kurita, T., Noda, Y., Takagi, T., Osumi, M. & Yoda, K. Kre6 Protein Essential for Yeast Cell Wall β-1,6-Glucan Synthesis Accumulates at Sites of Polarized Growth. *J. Biol. Chem.* 286, 7429–7438 (2011).

97. Kroth, P. G. *et al.* A Model for Carbohydrate Metabolism in the Diatom *Phaeodactylum tricornutum* Deduced from Comparative Whole Genome Analysis. *PLOS ONE* 3, e1426 (2008).

98. Huang, W., Río Bártulos, C. & Kroth, P. G. Diatom Vacuolar 1,6-β-Transglycosylases can Functionally Complement the Respective Yeast Mutants. *J. Eukaryot. Microbiol.* 63, 536–546 (2016).

99. Inukai, M. *et al.* Kre6 (yeast 1,6-β-transglycosylase) homolog, PhTGS, is essential for β-glucan synthesis in the haptophyte *Pleurochrysis haptonemofera*. *Front. Bioeng. Biotechnol.* 11, 1259587 (2023).

100. Kurita, T., Noda, Y. & Yoda, K. Action of multiple endoplasmic reticulum chaperon-like proteins is required for proper folding and polarized localization of Kre6 protein essential in yeast cell wall β-1,6-glucan synthesis. *J. Biol. Chem.* 287, 17415–17424 (2012).

101. Kubo, K. *et al.* Jerveratrum-Type Steroidal Alkaloids Inhibit β-1,6-Glucan Biosynthesis in Fungal Cell Walls. *Microbiol. Spectr.* 10, e00873-21.

102. Kitamura, A., Someya, K., Hata, M., Nakajima, R. & Takemura, M. Discovery of a Small-Molecule Inhibitor of β-1,6-Glucan Synthesis. *Antimicrob. Agents Chemother.* 53, 670–677 (2009).

103. Rai, L. S., Chauvel, M., Permal, E., d'Enfert, C. & Bachellier-Bassi, S. Transcript profiling reveals the role of PDB1, a subunit of the pyruvate dehydrogenase complex, in *Candida albicans* biofilm formation. *Res. Microbiol.* 174, 104014 (2023).

104. Z, L. *et al.* Conidium Specific Polysaccharides in *Aspergillus fumigatus*. *J. Fungi Basel Switz.* 9, (2023).

105. DuBois, Michel., Gilles, K. A., Hamilton, J. K., Rebers, P. A. & Smith, Fred. Colorimetric Method for Determination of Sugars and Related Substances. *Anal. Chem.* 28, 350–356 (1956).

106. Sawardeker, J. S., Sloneker, J. H. & Jeanes, Allene. Quantitative Determination of Monosaccharides as Their Alditol Acetates by Gas Liquid Chromatography. *Anal. Chem.* 37, 1602–1604 (1965).

107. Zverlov, V. V., Volkov, I. Y., Velikodvorskaya, T. V. & Schwarz, W. H. Highly thermostable endo-1,3-beta-glucanase (laminarinase) LamA from *Thermotoga neapolitana*: nucleotide sequence of the gene and characterization of the recombinant gene product. *Microbiol. Read. Engl.* 143 (Pt 5), 1701–1708 (1997).

108. Dueñas-Santero, E. *et al.* Characterization of Glycoside Hydrolase Family 5 Proteins in *Schizosaccharomyces pombe*. *Eukaryot. Cell* 9, 1650–1660 (2010).

109. Fontaine, T., Hartland, R. P., Beauvais, A., Diaquin, M. & Latge, J.-P. Purification and Characterization of an Endo-1,3-β-Glucanase from *Aspergillus fumigatus*. *Eur. J. Biochem.* 243, 315–321 (1997).

110. Vranken, W. F. *et al.* The CCPN data model for NMR spectroscopy: Development of a software pipeline. *Proteins Struct. Funct. Bioinforma.* 59, 687–696 (2005).

111. Ancian, B., Bourgeois, I., Dauphin, J.-F. & Shaw, A. A. Artifact-Free Pure Absorption PFG-Enhanced DQF-COSY Spectra Including a Gradient Pulse in the Evolution Period. *J. Magn. Reson.* 125, 348–354 (1997).

112. Thrippleton, M. J. & Keeler, J. Elimination of Zero-Quantum Interference in Two-Dimensional NMR Spectra. *Angew. Chem. Int. Ed.* 42, 3938–3941 (2003).

113. Willker, W., Leibfritz, D., Kerssebaum, R. & Bermel, W. Gradient selection in inverse heteronuclear correlation spectroscopy. *Magn. Reson. Chem.* 31, 287–292 (1993).

114. Kay, L. E., Keifer, P. & Saarinen, T. Pure absorption gradient enhanced heteronuclear single quantum correlation spectroscopy with improved sensitivity. *J. Am. Chem. Soc.* 114, 10663–10665 (1992).

115. Enthart, A., Freudenberger, J. C., Furrer, J., Kessler, H. & Luy, B. The CLIP/CLAP-HSQC: Pure absorptive spectra for the measurement of one-bond couplings. *J. Magn. Reson.* 192, 314–322 (2008).

116. Nyberg, N. T., Duus, J. Ø. & Sørensen, O. W. Heteronuclear Two-Bond Correlation: Suppressing Heteronuclear Three-Bond or Higher NMR Correlations while Enhancing Two-Bond Correlations Even for Vanishing 2JCH. *J. Am. Chem. Soc.* 127, 6154–6155 (2005).

117. Cicero, D. O., Barbato, G. & Bazzo, R. Sensitivity enhancement of a two-dimensional experiment for the measurement of heteronuclear long-range coupling constants, by a new scheme of coherence selection by gradients. *J. Magn. Reson. San Diego Calif 1997* 148, 209–213 (2001).

118. Baquero, D. P. *et al.* A filamentous archaeal virus is enveloped inside the cell and released through pyramidal portals. *Proc. Natl. Acad. Sci.* 118, e2105540118 (2021).

119. Hall, R. A. *et al.* The Mnn2 mannosyltransferase family modulates mannoprotein fibril length, immune recognition and virulence of *Candida albicans*. *PLoS Pathog.* 9, e1003276 (2013).

120. Matveev, A. L. *et al.* Novel mouse monoclonal antibodies specifically recognizing β-(1→3)-D-glucan antigen. *PloS One* 14, e0215535 (2019).

121. Wong, S. S. W. *et al.* Differential Interactions of Serum and Bronchoalveolar Lavage Fluid Complement Proteins with Conidia of Airborne Fungal Pathogen *Aspergillus fumigatus*. *Infect. Immun.* 88, e00212-20 (2020).

122. Vyas, V. K., Barrasa, M. I. & Fink, G. R. A *Candida albicans* CRISPR system permits genetic engineering of essential genes and gene families. *Sci. Adv.* 1, e1500248 (2015).

123. Min, K., Ichikawa, Y., Woolford, C. A. & Mitchell, A. P. *Candida albicans* Gene Deletion with a Transient CRISPR-Cas9 System. *mSphere* 1, e00130-16 (2016).

124. Reuss, O., Vik, A., Kolter, R. & Morschhäuser, J. The SAT1 flipper, an optimized tool for gene disruption in *Candida albicans*. *Gene* 341, 119–127 (2004).

125. Basso, L. R. *et al.* Transformation of *Candida albicans* with a synthetic hygromycin B resistance gene. *Yeast Chichester Engl.* 27, 1039–1048 (2010).

126. Sanglard, D., Ischer, F., Monod, M. & Bille, J. Susceptibilities of *Candida albicans* multidrug transporter mutants to various antifungal agents and other metabolic inhibitors. *Antimicrob. Agents Chemother.* 40, 2300–2305 (1996).

127. Chauvel, M. *et al.* High-throughput functional profiling of the human fungal pathogen *Candida albicans* genome. *Res. Microbiol.* 174, 104025 (2023).

128. Chauvel, M. *et al.* A versatile overexpression strategy in the pathogenic yeast *Candida albicans*: identification of regulators of morphogenesis and fitness. *PloS One* 7, e45912 (2012).

129. Legrand, M. *et al.* Generating genomic platforms to study *Candida albicans* pathogenesis. *Nucleic Acids Res.* 46, 6935–6949 (2018).

130. Vogt, M. S., Schmitz, G. F., Varón Silva, D., Mösch, H.-U. & Essen, L.-O. Structural base for the transfer of GPI-anchored glycoproteins into fungal cell walls. *Proc. Natl. Acad. Sci. U. S. A.* 117, 22061–22067 (2020).

Figures

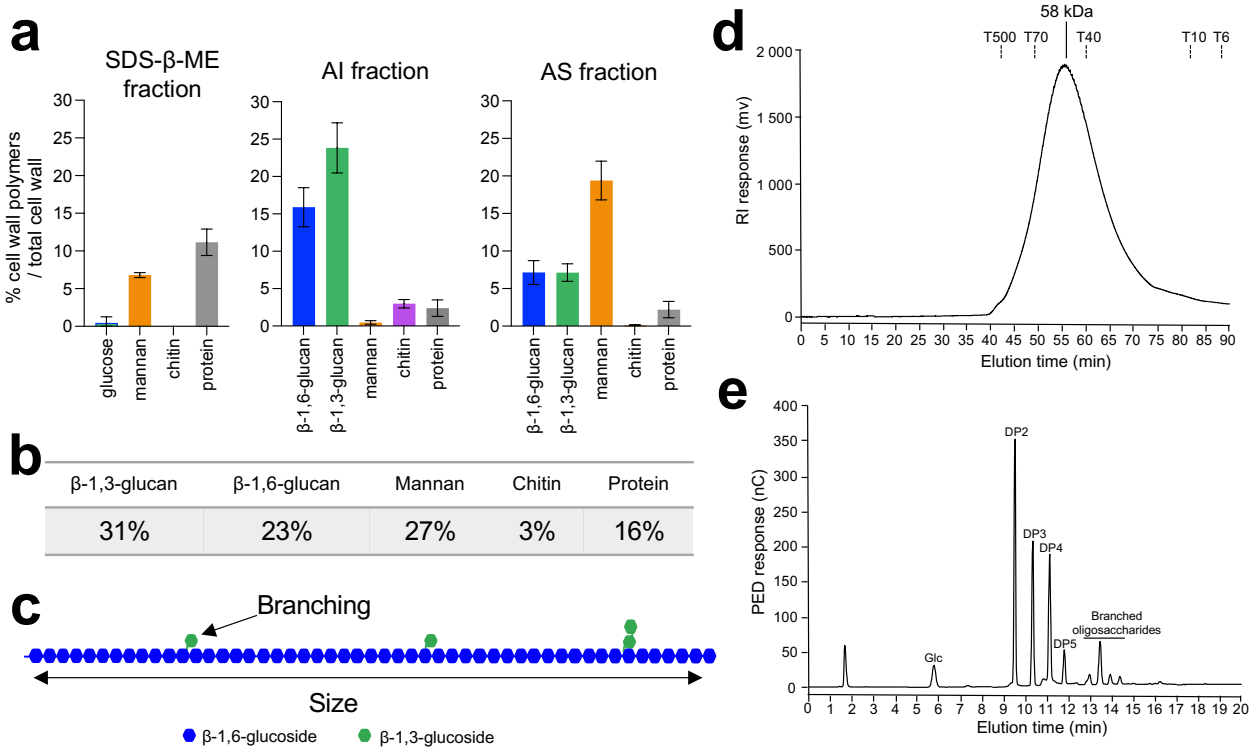

Figure 1: Analysis of *C. albicans* cell wall β-1,6-glucans.

a, Percentages of cell wall polymers on total cell wall, distributed by fractions: SDS-β-ME, AI and AS. Cells were grown in SD medium at 37°C. Means and standard deviations were calculated from three independent experiments. **b**, Table of the mean percentages of each polymer in the cell wall from three independent experiments. **c**, Diagram of β-1,6-glucan structure. In blue are represented glucose residues linked in β-1,6 and in green glucose residues linked in β-1,3. According to NMR analysis and HPAEC after endo-β-1,6-glucanase digestion (Table S2), based on three independent experiments, an average of 6.4% (+/- 0.5%) of glucose units of the main chain are substituted by a single glucose residue (88-90%) or a laminaribiose (10-12%). **d**, Gel filtration analysis on a Superdex 200 column of β-1,6-glucan released by endo-β-1,3-glucanase digestion. The column was calibrated with dextrans (Tx: x kDa). **e**, HPAEC chromatographic analysis of the digestion products of the AI fraction treated with an endo-β-1,6-glucanase. Chromatographs in d and e are representative of three independent experiments. *PED*, pulsed electrochemical detector; *nC*, nanocoulombs; *RI*, refractive index; *mV*, millivolt; DP, degree of polymerization; Glc, glucose.

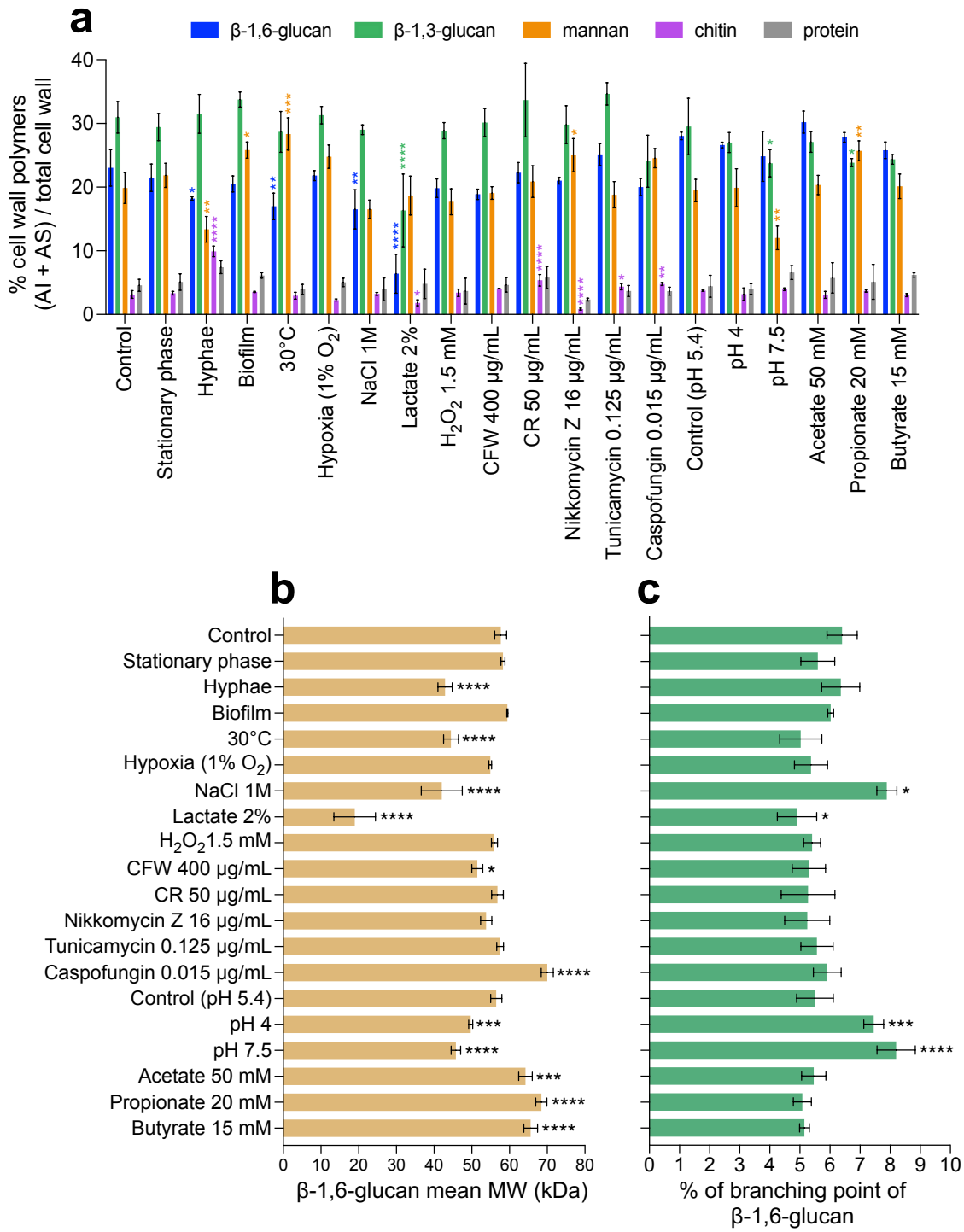

Figure 2: Comparative analyses of cell wall β-1,6-glucans produced in various environmental conditions.

a, Percentages of cell wall polymers (AI + AS fractions) on total cell wall. Cells were grown in liquid synthetic medium at 37°C under different conditions, as specified in Methods. **b**, β-1,6-glucan mean molecular weight (MW). Average molecular weight was estimated by gel filtration chromatography on a Superdex 200 column. **c**, Branching rate of β-1,6-glucans. Branching rate was determined by HPAEC after digestion of the AI fraction by an endo-β-1,6-glucanase (% expressed as number of glucose units of the main chain that are substituted by a side chain).

For a, b, and c, means and standard deviations from three independent replicate experiments are shown. All data were compared to the control conditions and were analysed by one-way ANOVA with Dunnett's multiple comparisons test: *, $P < 0,05$; **, $P < 0,01$; ***, $P < 0,001$; ****, $P < 0,0001$.

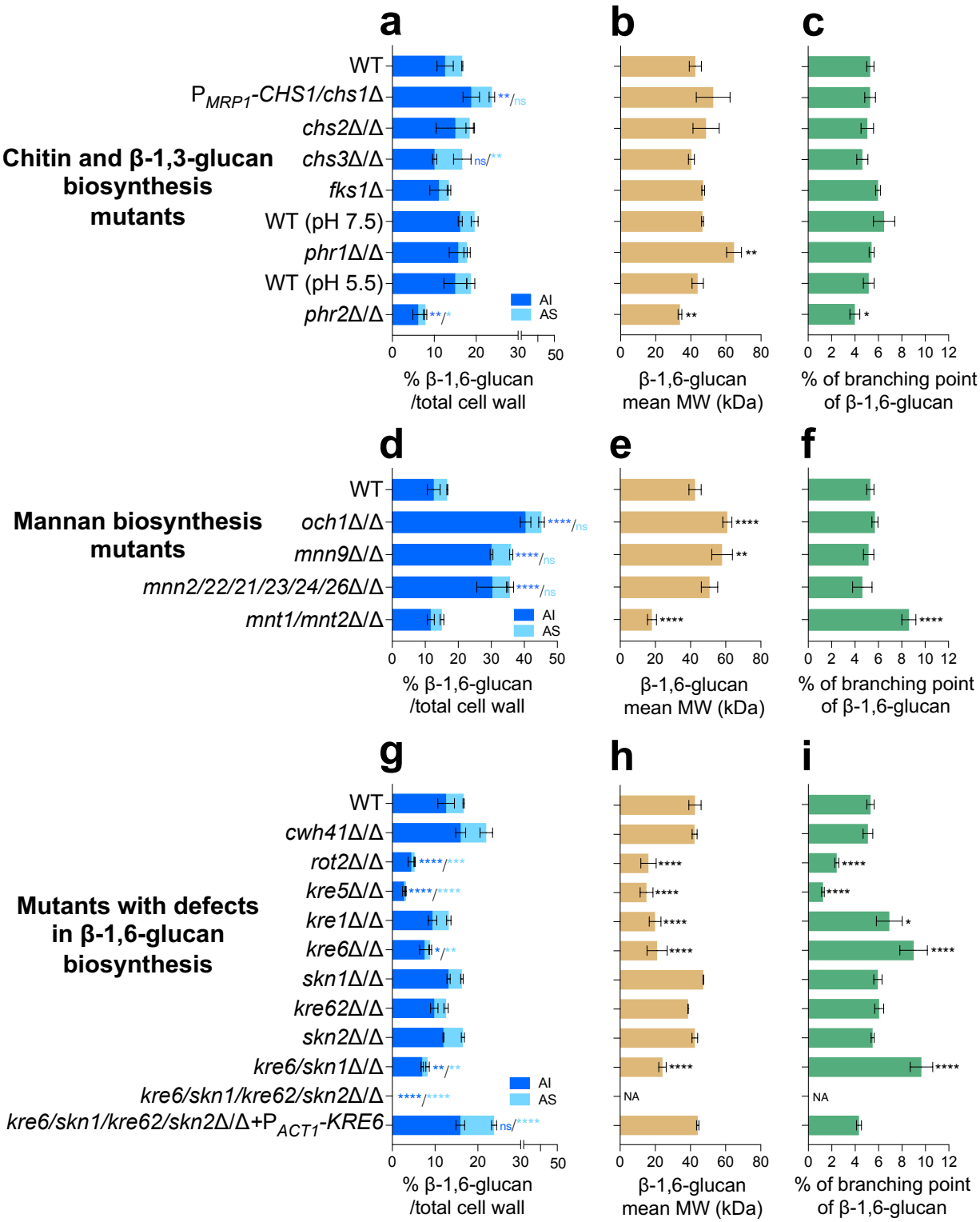

Figure 3: Comparative analysis of β-1,6-glucan content and structure produced by cell wall mutants.

a, **d, g** Percentages of cell wall β-1,6-glucans (AI and AS fractions) on total cell wall. **b**, **e**, **h**, β-1,6-glucans mean molecular weight (MW) and **c**, **f**, **i** Branching rate of β-1,6-glucans.

Cells were grown in liquid SD medium at 30°C. Means and standard deviations from three independent replicate experiments are shown. All data were compared to the control conditions and

were analysed by one-way ANOVA with Dunnett's multiple comparisons test: *, $P < 0,05$; **, $P < 0,01$; ***, $P < 0,001$; ****, $P < 0,0001$; ns: non-significant; NA: non-applicable.

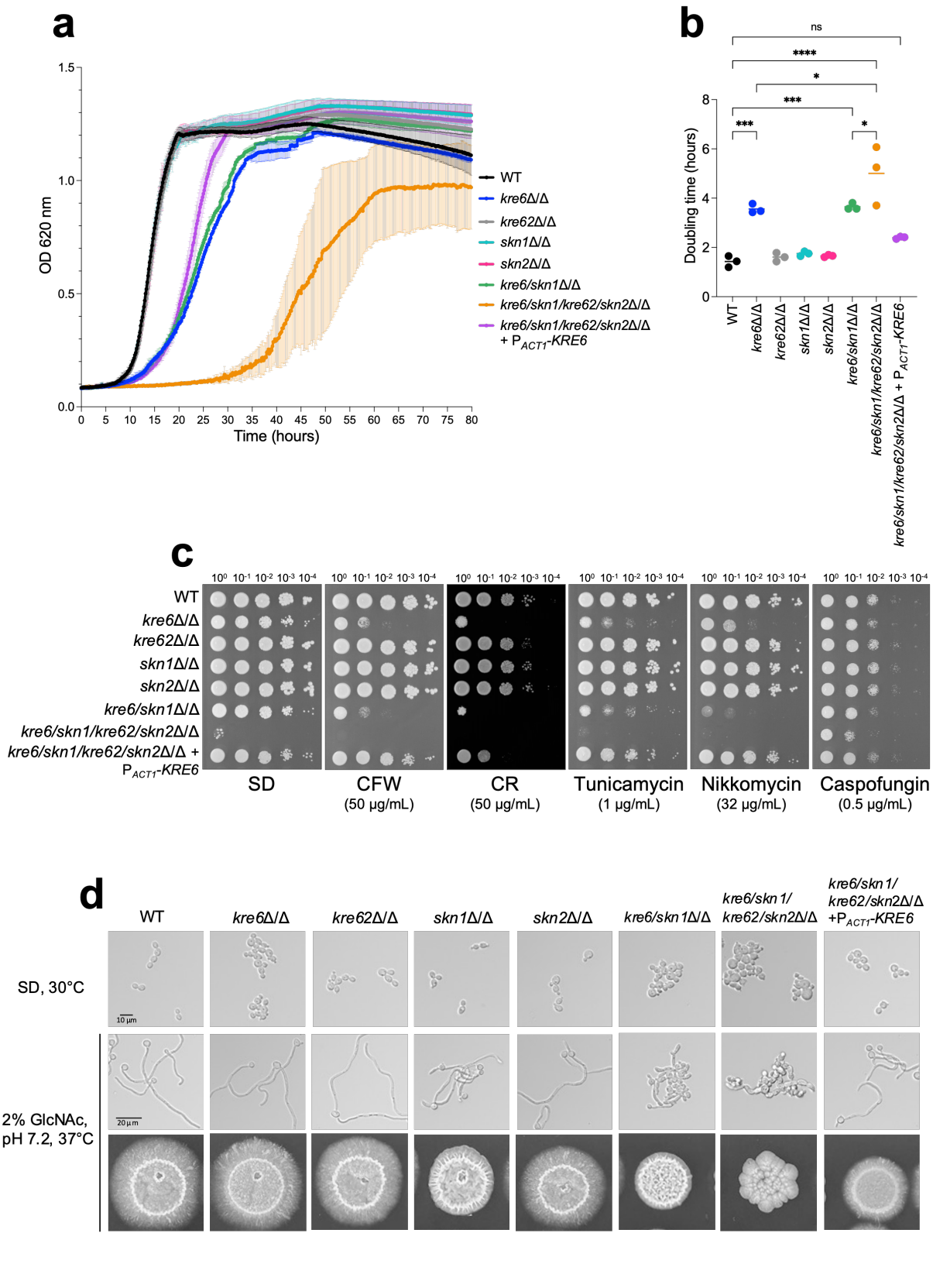

Figure 4: Phenotypic characterization of *KRE6* family mutants: growth kinetics, drug susceptibility and filamentation.

a, Kinetic curve of all strains grown in liquid SD medium, 30°C. Optical density at 620 nm was measured every 10 min during 80 hours by TECAN SUNRISE. Means and standard deviations were calculated from three independent experiments.

b, Doubling time of each strain was determined from three independent replicates. Statistical analyses were performed with one-way ANOVA with Tukey's multiple comparisons test: *, $P < 0,05$; **, $P < 0,01$; ***, $P < 0,001$; ****, $P < 0,0001$; ns: non-significant.

c, Spotting test of 10-fold serial dilution of yeast cells of all strains on SD medium, 30°C, 48h, with cell wall disturbing agents (CR, Congo red; CFW, CalcoFluor White) or drugs (nikkomycin, tunicamycin, caspofungin). These results are representative of three independent experiments. Pictures were taken with a Phenobooth (Singer Instruments).

d, Filamentation assay of all strains. Top row, growth in liquid SD medium at 30°C; middle panels: growth in liquid YNB medium + 2% GlcNAc, buffered at pH 7.2 at 37°C during 6h. Picture were taken using an Olympus IX 83 microscope, 40x objective. Bottom row, cells were grown on agar YNB + 2% GlcNAc, buffered at pH 7.2, at 37°C for 6 days.

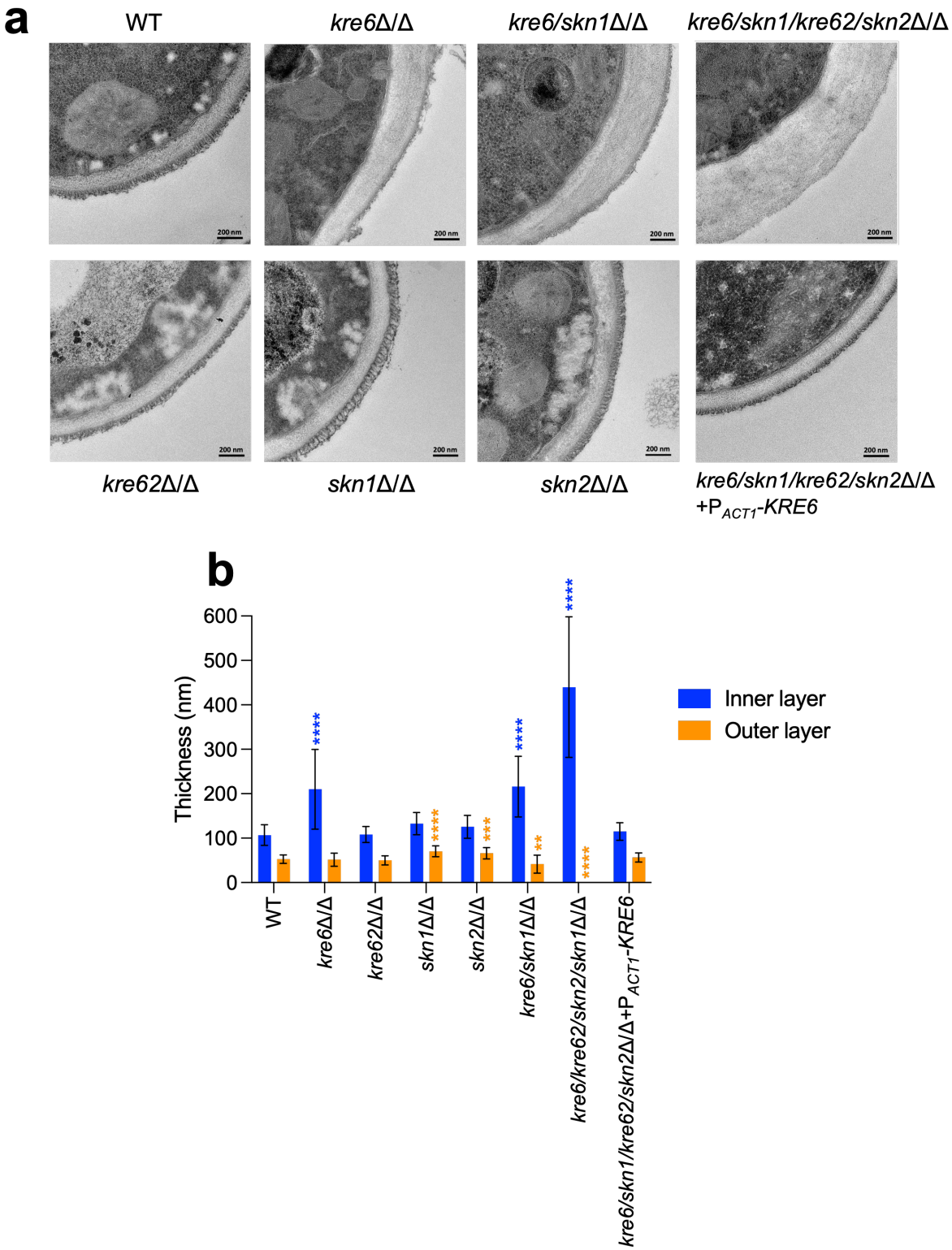

Figure 5: Cell wall electron microscopy observations of *KRE6* simple and multiple mutants.

a, Representative transmission electron microscopy images of the cell wall of each strains. After culture, cells were fixed and high-pressure frozen and freeze substituted with Spurr resin. Sections were cut and stained and then pictures were taken by a Tecnai Spirit 120Kv TEM microscope. Scale bar= 200 nm.

b, Measurement of the inner and outer cell wall layers of the mutants. Means and standard deviations are represented. 37-40 measurements were performed randomly on 7-13 cells.

Statistical analyses were performed with one-way ANOVA with Tukey's multiple comparisons test: *, $P < 0,05$; **, $P < 0,01$; ***, $P < 0,001$; ****, $P < 0,0001$.

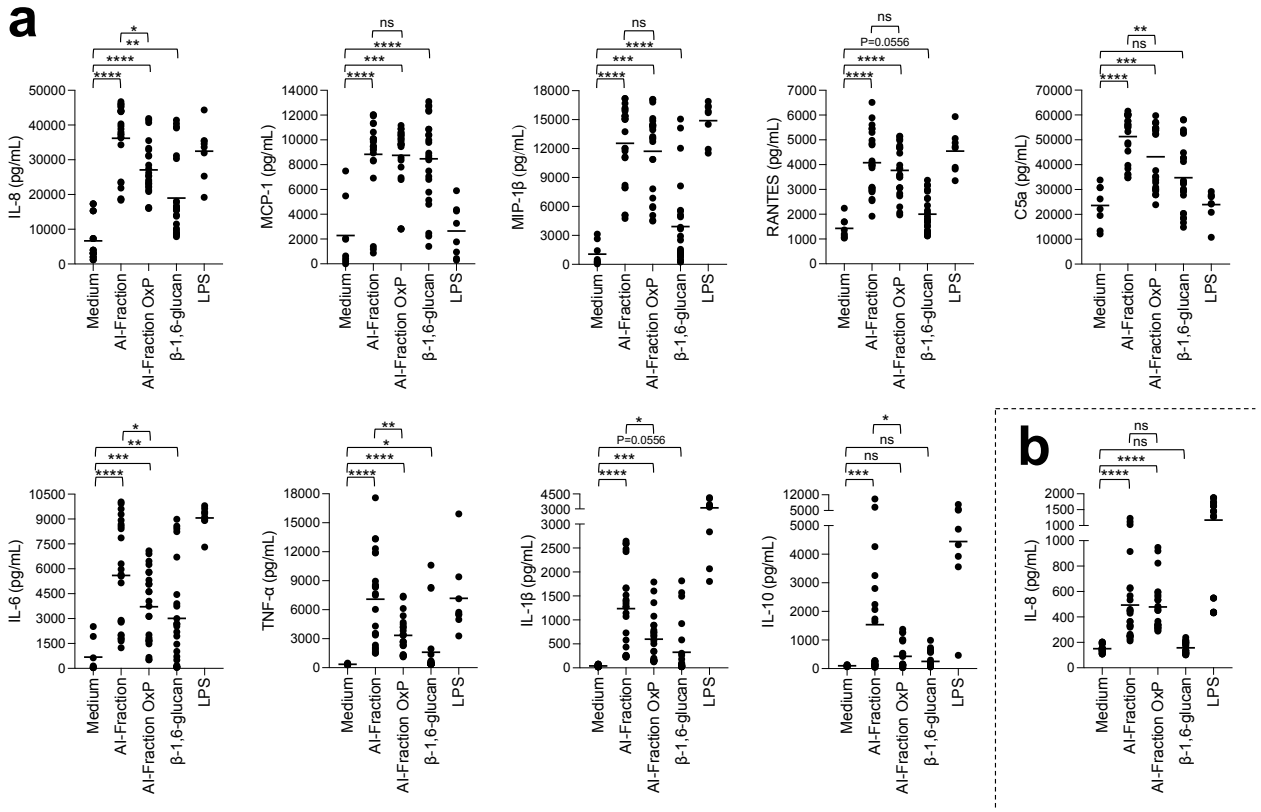

Figure 6: Stimulation of PBMCs and neutrophils *in vitro* by cell wall fractions and purified β-1,6-glucans from *C. albicans*.

Cytokines, chemokines or acute phase proteins (IL-8, MCP-1, IL-6, MIP-1β, IL-1β, TNF-α, RANTES, C5a, IL-10) concentrations in culture supernatants of PBMCs (**a**) and neutrophils (**b**) stimulated by cell wall fractions of *C. albicans* (AI-Fraction, AI-Fraction OxP and β-1,6-glucan) at 25 µg/mL or LPS (positive control, 0.1 µg/mL). PBMC cells and neutrophils were isolated from healthy human donors (n=8). Three independent batches of each fractions were used. Means are represented and data were analyzed using nonparametric Friedman test with Dunn's multiple comparisons: *, $P < 0,05$; **, $P < 0,01$; ***, $P < 0,001$; ****, $P < 0,0001$; ns: non-significant.

a

C. albicans cell wall structure

β-1,6-glucan is a major cell wall component and important for cell wall integrity

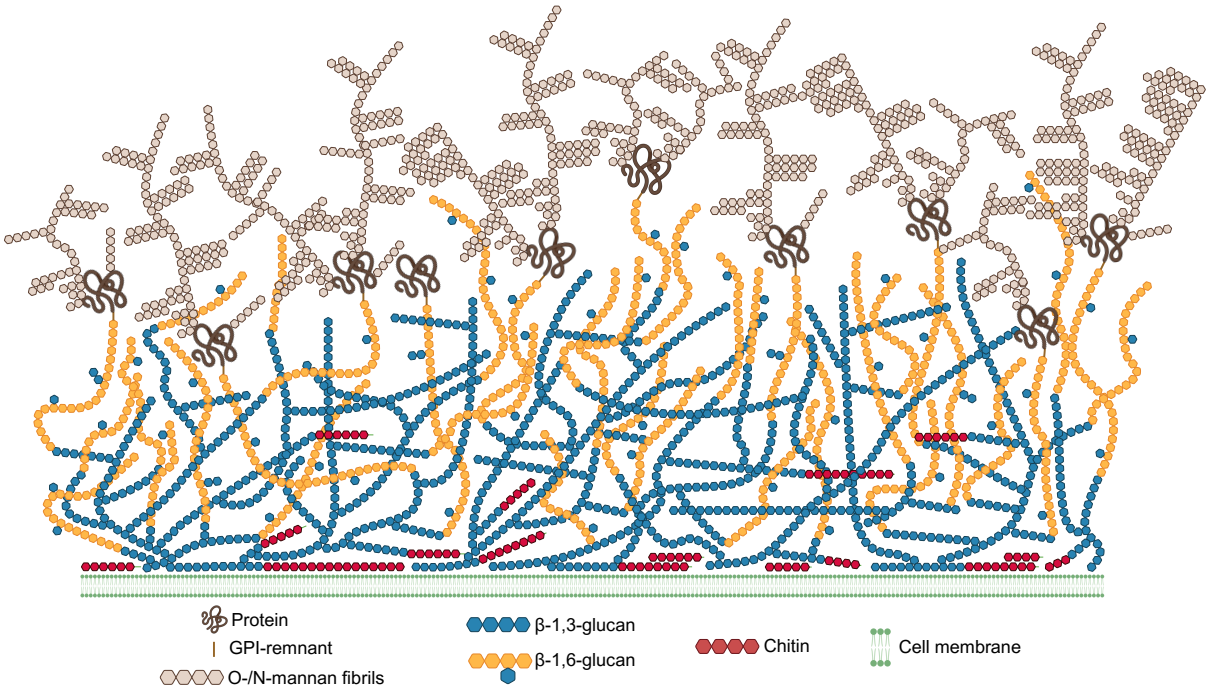

b

β-1,6-glucan dynamic is dependent on environmental conditions

In terms of content and structure (size, branching)

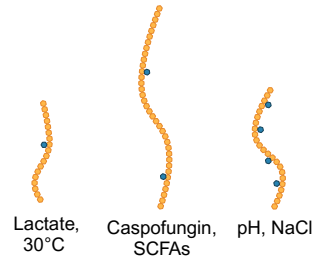

c

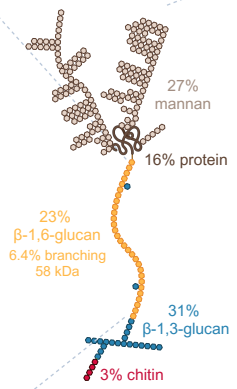

β-1,6-glucan biosynthesis is a compensatory pathway to O-/N-mannan elongation defects

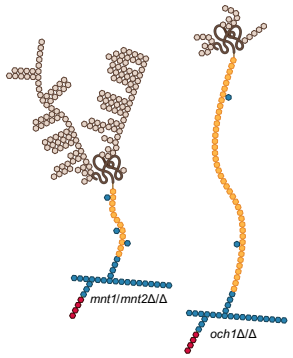

d

β-1,6-glucan is immunostimulatory on PBMCs from healthy human donors

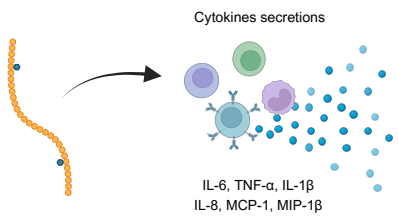

e

Absence of β-1,6-glucan in *C. albicans* after deletion of *KRE6* family genes

Cell wall remodelling and fibrillar outer layer loss

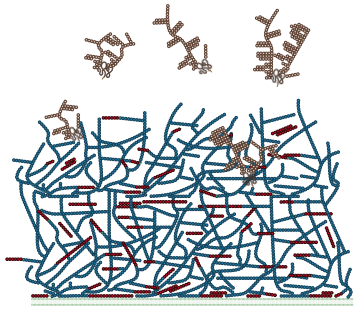

kre6/*kre62*/*skn2*/*skn1*Δ/Δ cell wall

Figure 7: β-1,6-glucan in *C. albicans* is a major and dynamic cell wall polymer.

a, Scheme of the cell wall of *C. albicans*. The proportion of each cell wall polymer was representative the results obtained on *C. albicans* SC5314 grown in liquid SD medium at 37°C. **b,** Scheme representing the dynamic of β-1,6-glucan under different environmental factors. **c**, β-1,6-glucan is a compensatory pathway for mannan elongation defect. **d**, β-1,6-glucan is a PAMP. **e**, Scheme of the cell wall of *KRE6* family deficient mutant.

Supplementary Figures

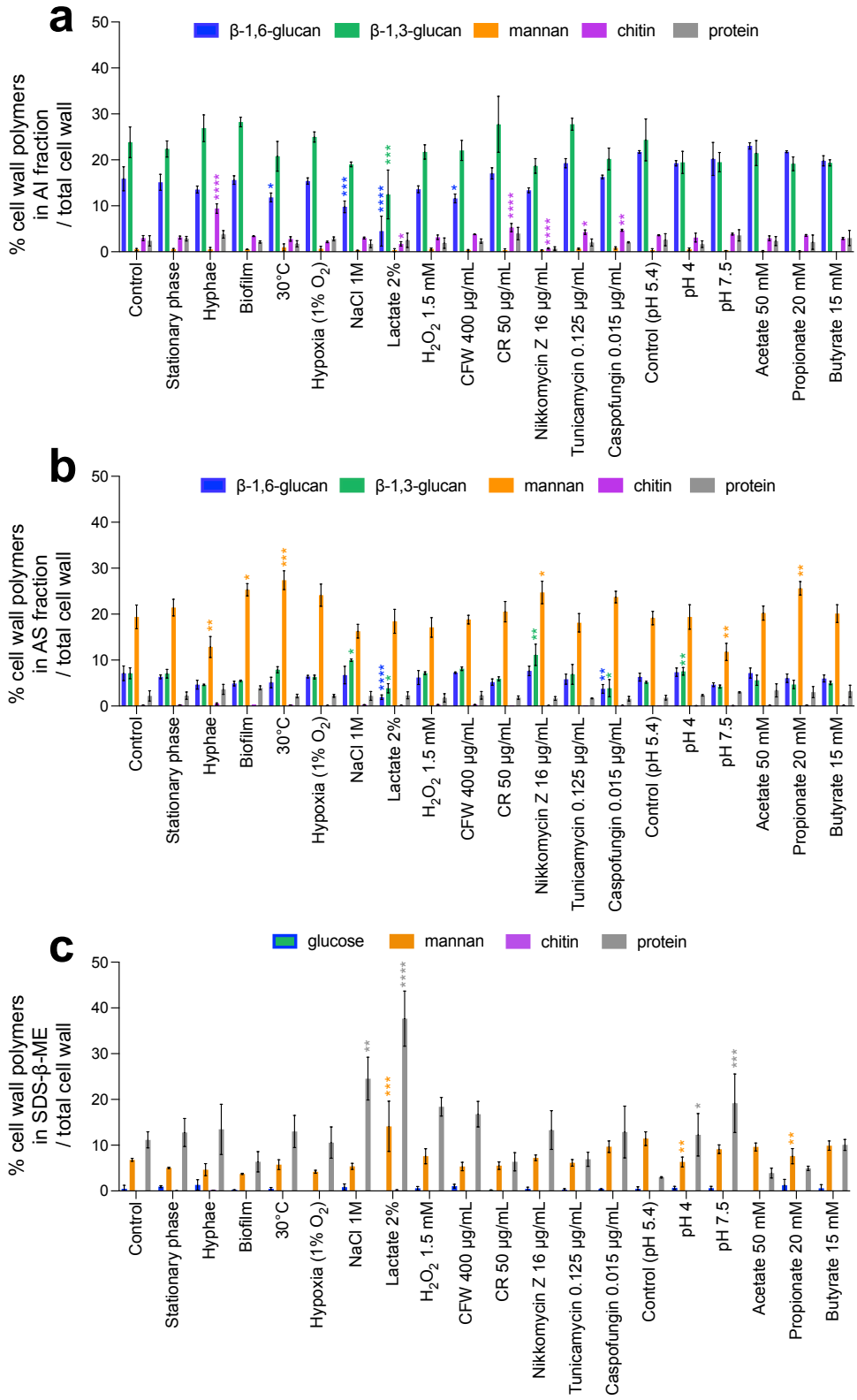

Figure S1: Global cell wall composition produced by *C. albicans* in different environmental conditions.

Results are represented as the percentage of each polymer on total cell wall in AI fraction (**a**), AS fraction (**b**) and SDS-β-ME fraction (**c**). Means and standard deviations were obtained from three independent replicate experiments. All data were compared to the control conditions and were

analysed using one-way ANOVA with Dunnett's multiple comparisons test: *, $P < 0,05$; **, $P < 0,01$; ***, $P < 0,001$; ****, $P < 0,0001$.

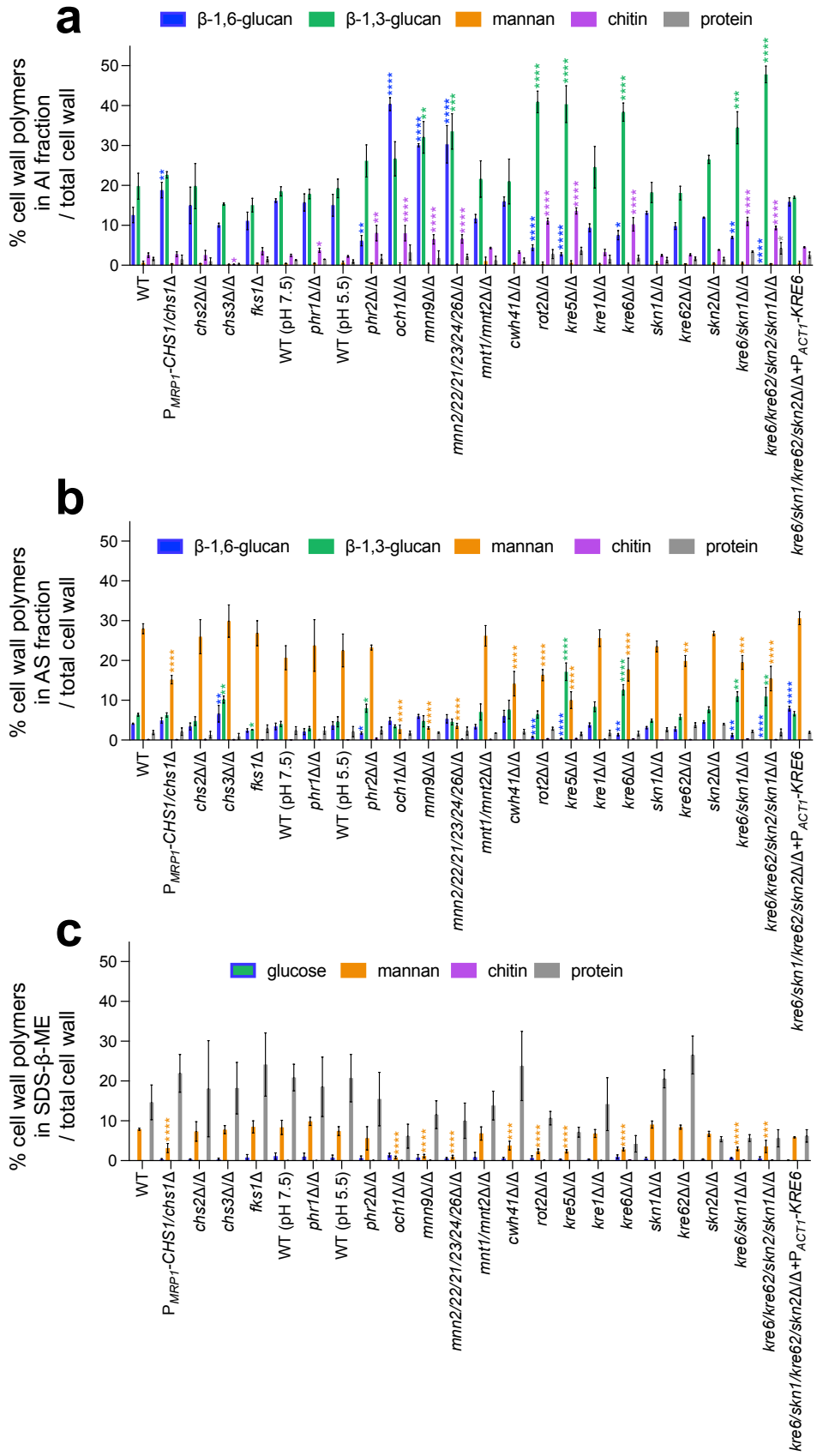

Figure S2: Cell wall composition of *C. albicans* mutants.

Results are represented as the percentage of each polymer on total cell wall in AI fraction (**a**), AS fraction (**b**), and SDS-β-ME fraction (**c**). Means and standard deviations were obtained from three independent replicate experiments. All data were compared to the parental strain SC5314 and were

analysed using one-way ANOVA with Dunnett's multiple comparisons test: *, $P < 0,05$; **, $P < 0,01$; ***, $P < 0,001$; ****, $P < 0,0001$.

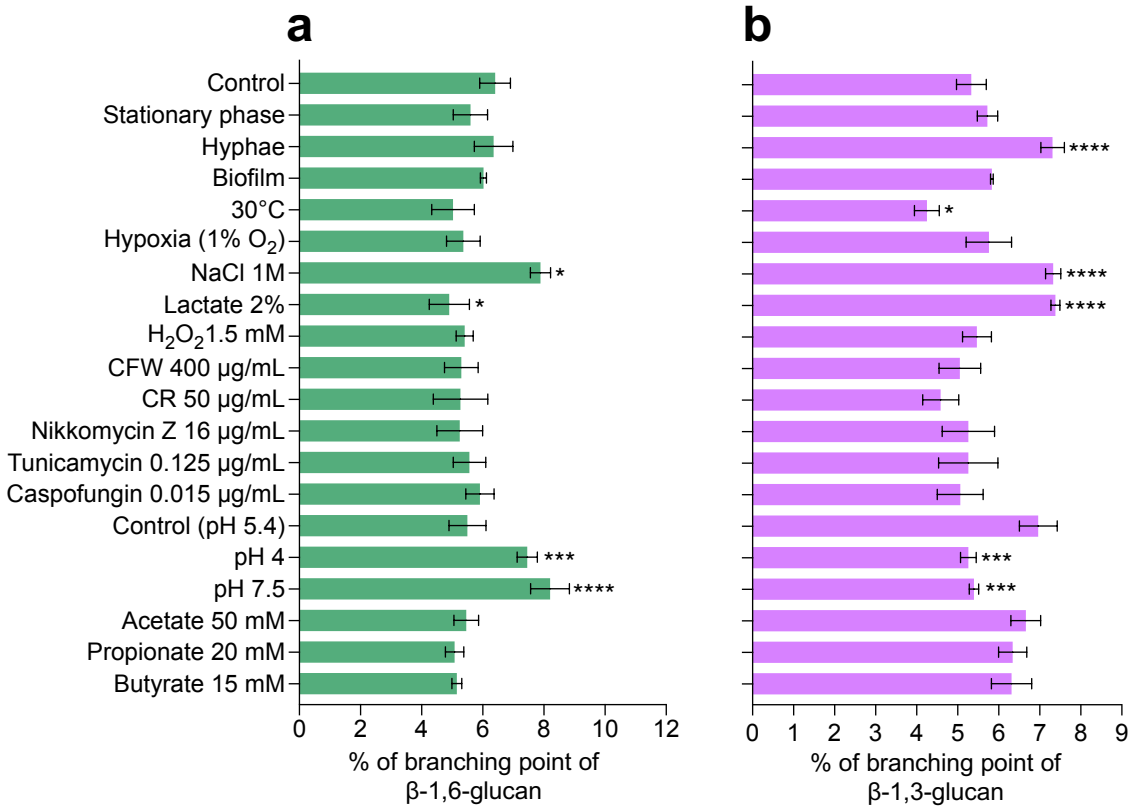

Figure S3: Branching rates of β-1,6-glucans and β-1,3-glucans produced by *C. albicans* under various environmental conditions.

a, Branching rate of β-1,6-glucans from AI fraction. The branching rate was estimated by HPAEC after digestion by an endo-β-1,6-glucanase.

b, Branching rate of β-1,3-glucans from AI fraction, The branching rate was estimated by HPAEC after digestion by an endo-β-1,3-glucanase.

Means and standard deviations from three independent replicate experiments are shown. All data were compared to the control conditions and were analysed using one-way ANOVA with Dunnett's multiple comparisons test: *, $P < 0,05$; **, $P < 0,01$; ***, $P < 0,001$; ****, $P < 0,0001$.

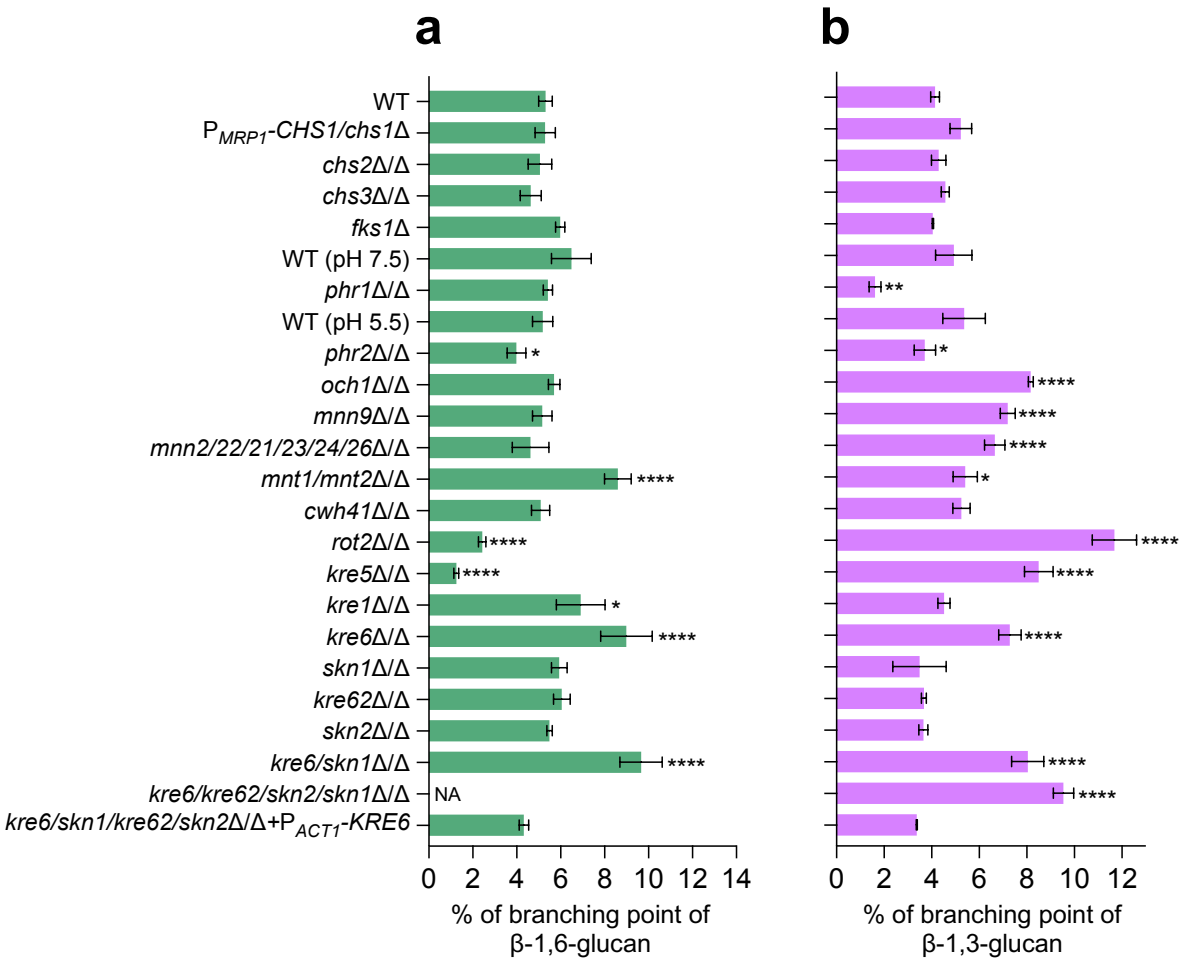

Figure S4: Branching rates of β-1,6-glucans and β-1,3-glucans produced by different cell wall mutants of *C. albicans.*

a, Branching rate of β-1,6-glucans from AI fraction. The branching rate was estimated by HPAEC after digestion by an endo-β-1,6-glucanase.

b, Branching rate of β-1,3-glucans from AI fraction. The branching rate was estimated by HPAEC after digestion by an endo-β-1,3-glucanase.

Means and standard deviations from three independent replicate experiments are shown. All data were compared to the control conditions and were analysed using one-way ANOVA with Dunnett's multiple comparisons test: *, $P < 0,05$; **, $P < 0,01$; ***, $P < 0,001$; ****, $P < 0,0001$; NA: non-applicable.

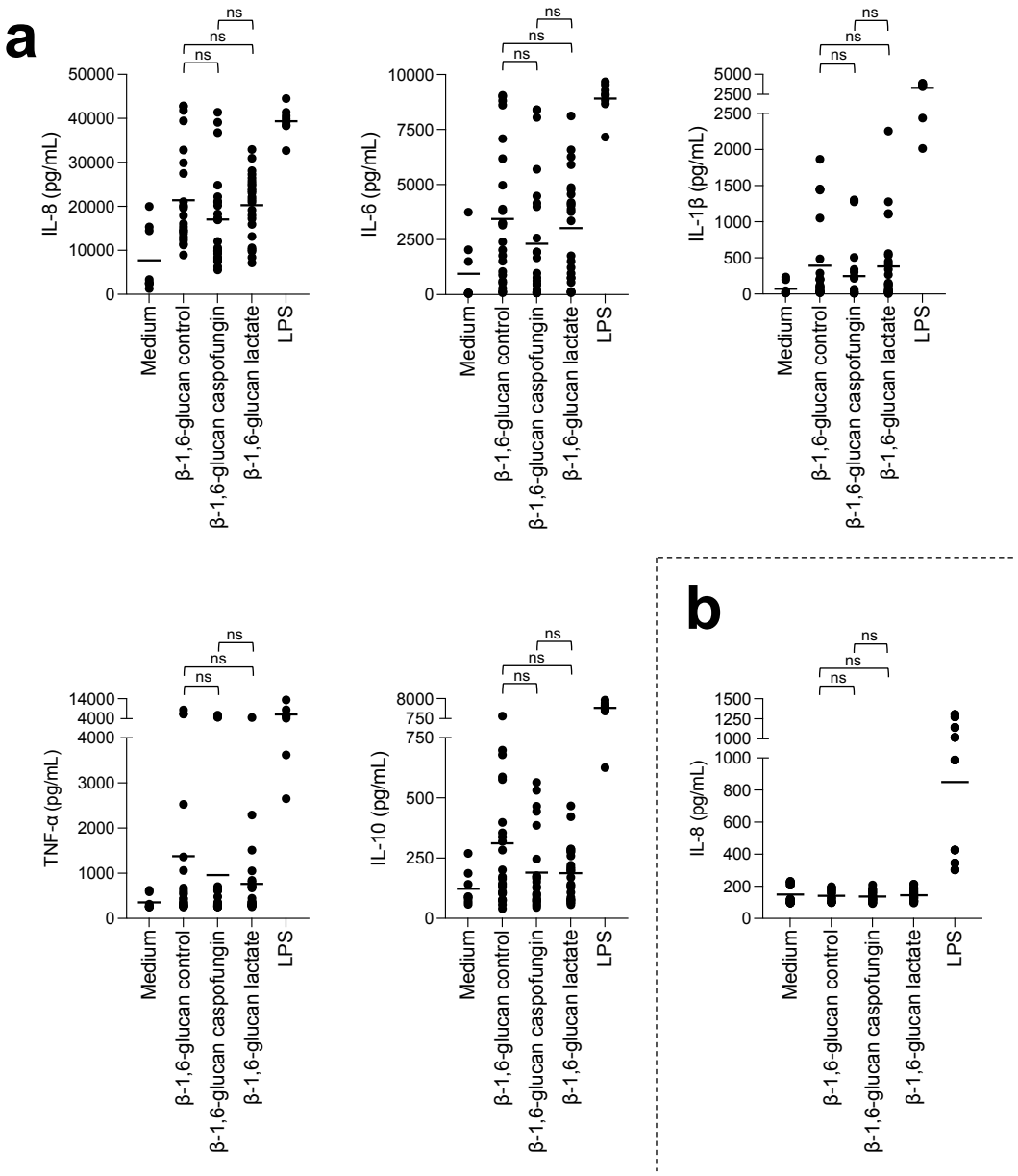

Figure S5: Stimulation of PBMCs and neutrophils *in vitro* by β-1,6-glucan with different size from *C. albicans.*

Cytokines, chemokines or acute phase proteins (IL-8, MCP-1, IL-6, MIP-1β, IL-1β, TNF-α, RANTES, C5a, IL-10) concentrations in culture supernatants of PBMCs (**panel a**) or neutrophils (**panel b**) stimulated by different β-1,6-glucans from *C. albicans* at 25 µg/mL or LPS (positive control, 0.1 µg/mL). β-1,6-glucans were isolated from cell wall AI fraction of *C. albicans* grown either at 37°C in SD medium (control, β-1,6-glucan size= 58 kDa), or in the presence of caspofungin at sublethal concentration 0.015 µg/mL (β-1,6-glucan size= 70 kDa) or in the presence of 2% lactate as sole carbon source (β-1,6-glucan size= 19 kDa). PBMCs and neutrophils were isolated from healthy human donors (n=8). Three independent batches of the different fractions were used. Means are represented and data were analyzed using nonparametric Friedman test with Dunn's multiple comparisons: ns: non-significant.

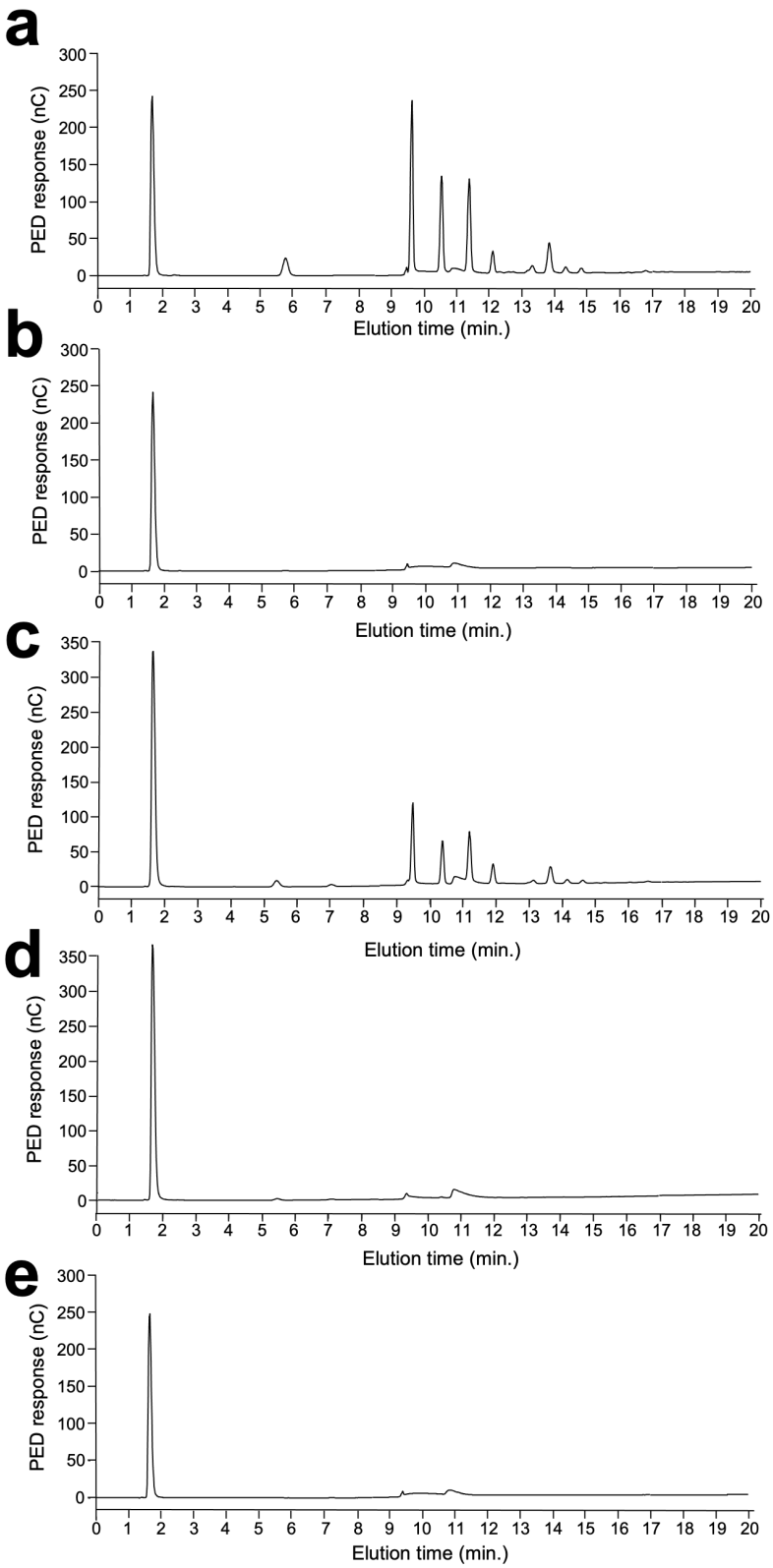

Figure S6: Absence of β-1,6-glucans in the cell wall of the quadruple *kre6/kre62/skn2/skn1*Δ/Δ mutant.

HPAEC analysis of oligosaccharides released by the endo-β-(1,6)-glucanase digestions of AI fraction of WT (**a**), AI fraction of *kre6/kre62/skn2/skn1*Δ/Δ (**b**), AS fraction of WT (**c**), AS fraction of

*kre6/kre62/skn2/skn1*Δ/Δ (**d**) and water (**e**). Experiments were performed in triplicates. *PED*, pulsed electrochemical detector; *nC*, nanocoulomb.

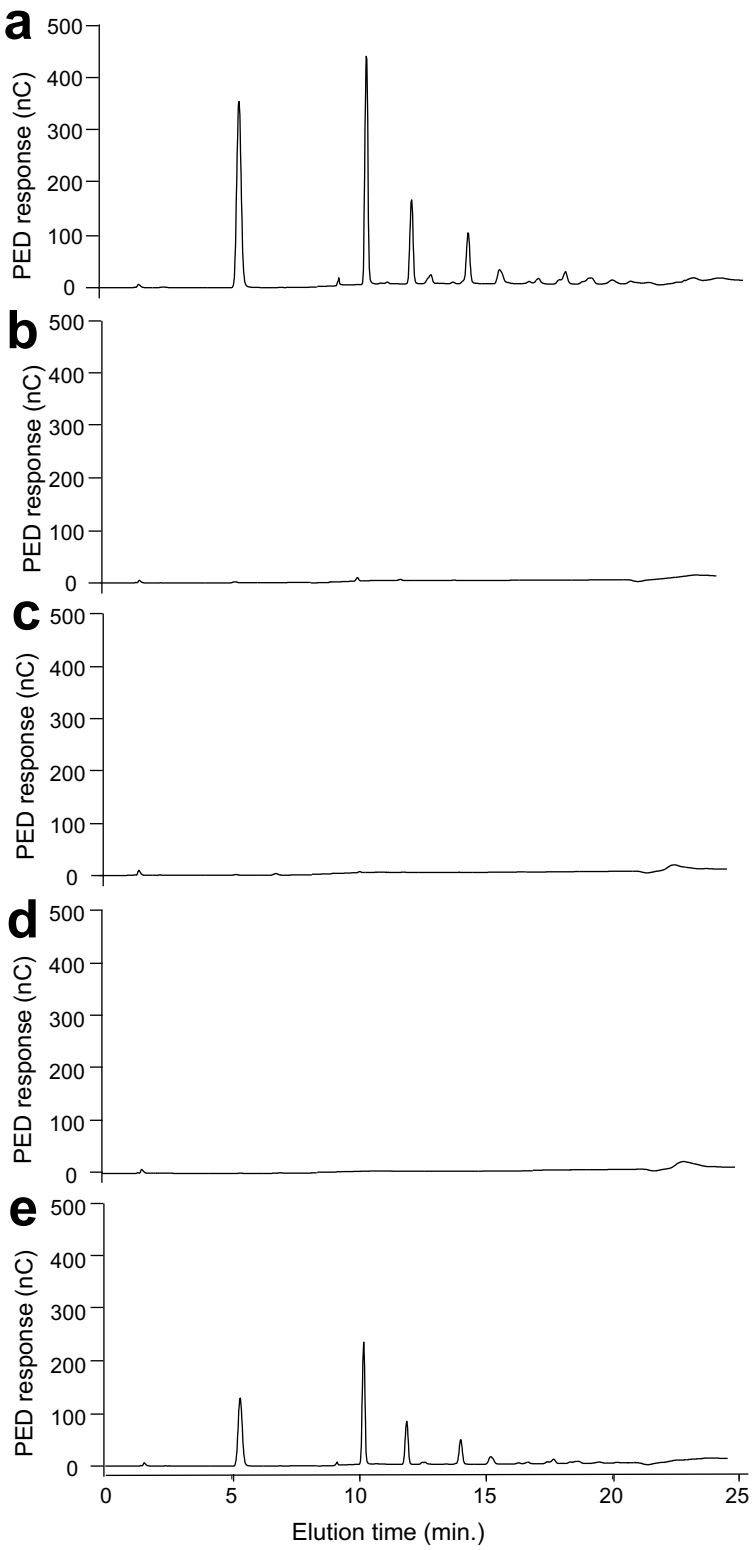

Figure S7: Cell disruption is essential to eliminate glycogen in AI and AS fractions.

HPAEC analysis of oligosaccharides released by α-amylase enzymatic digestion of AI and AS fractions.

(**a**) Control: glycogen, (**b**) AI fraction obtained after biomass cell disruption, (**c**) AI fraction from biomass with no cell disruption, (**d**) AS fraction obtained after biomass cell disruption, (**e**) AS fraction from biomass with no cell disruption. *PED*, pulsed electrochemical detector; *nC*, nanocoulomb.

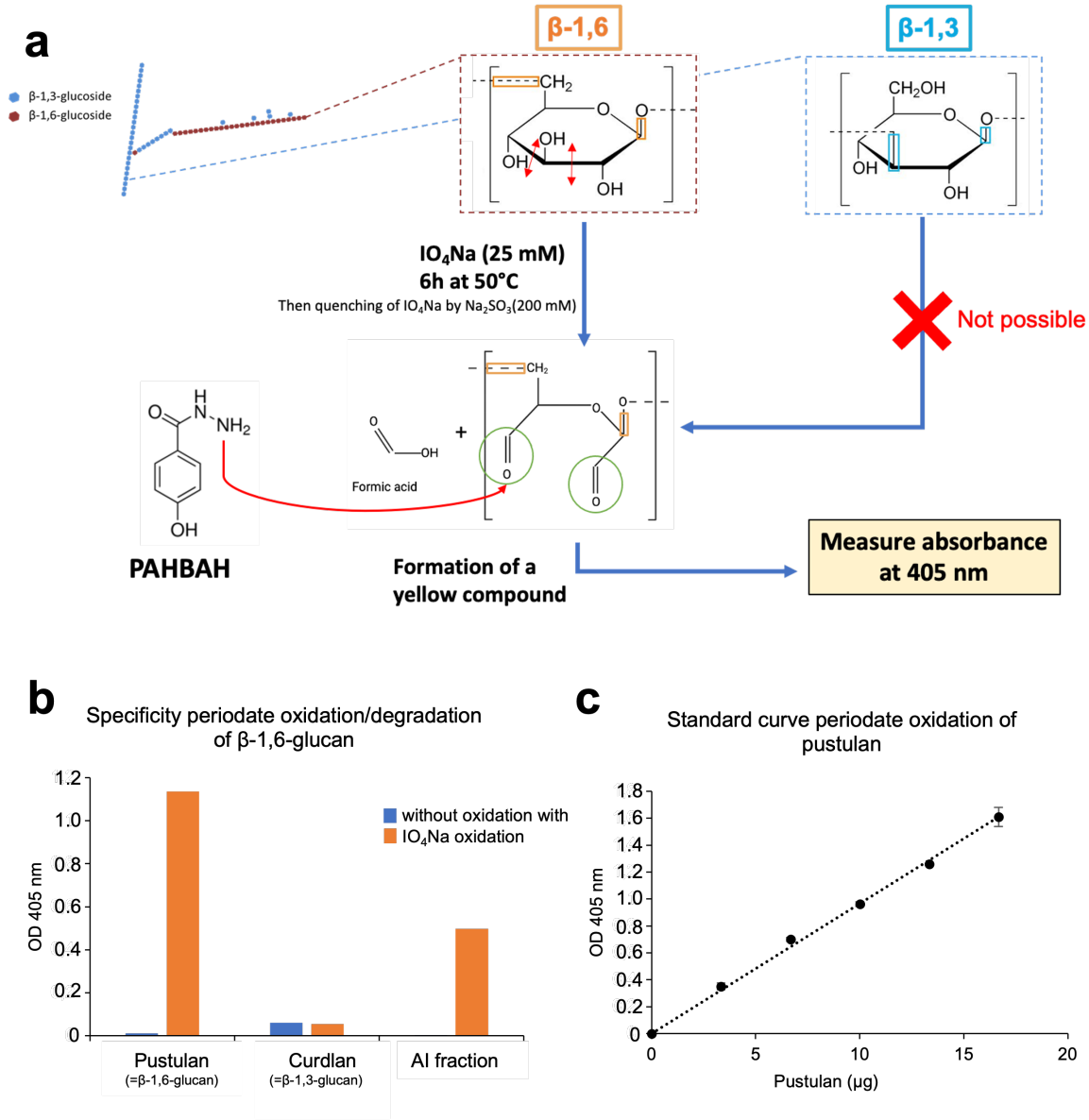

Figure S8: Quantification methods of β-1,6-glucans in AI fractions.

a, The specific oxidation of β-1,6-glucans of the AI fraction by periodate was used for quantification. Briefly, IO_4Na splits bonds between vivinal carbons bearing hydroxyl groups (only present in β-1,6-glucoside), which leads to the formation of aldehydes, which can react with 4-Hydroxybenzhydrazide (PAHBAH) to form a yellow compound measurable by absorbance at OD=405 nm.

b, Specificity of the periodate oxidation method for β-1,6-glucans (pustulan). The method is specific for β-1,6-glucans (pustulan and AI fraction) and inactive on β-1,3-glucans (curdlan).

c, Linearity of β-1,6-glucan assay after periodate oxidation. We showed that the response of the method described in (a) is proportional from 0 to 20 µg of pustulan.

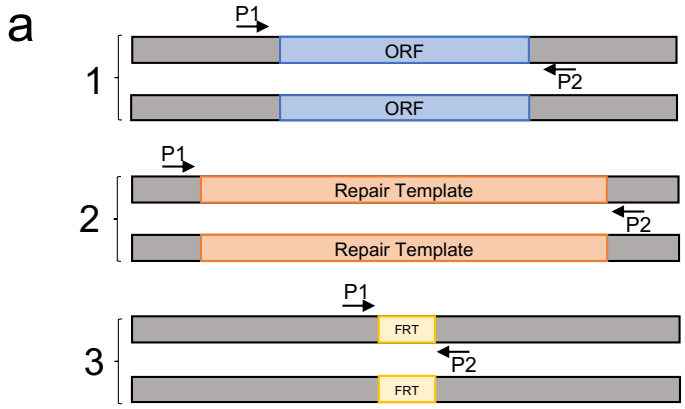

b

PCR band expected (in bp)	ORF=*KRE6*			ORF=*KRE62*			ORF=*SKN2*			ORF=*SKN1*		
	1	2	3	1	2	3	1	2	3	1	2	3
WT	2784			2307			2671			2483		
kre6Δ/Δ	2784	2642										
kre62Δ/Δ				2307	4592	506						
skn2Δ/Δ							2671	4668	582			
skn1Δ/Δ										2483	4423	337
kre6/skn1Δ/Δ	2784	2642								2483	4423	337
kre6/kre62/skn2/skn1Δ/Δ	2784	2642		2307	4592	506	2671	4668	582	2483	4423	337

c

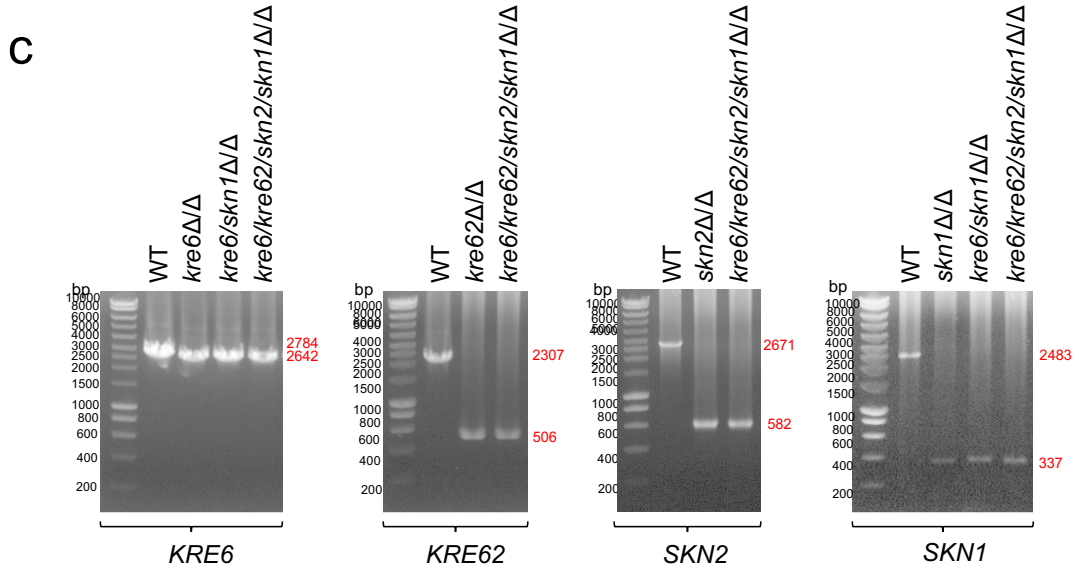

Figure S9: Control PCR control of mutants obtained in this study.

a, Principle of PCR check done in b and c. P1 and P2 are PCR diagnostic primers. ORF = *KRE6*, *KRE62*, *SKN2* or *SKN1*. Repair Templates contain either *HygB* or a *SAT1-Flipper* cassette for selection. FRT correspond to the scar after *SAT1-Flipper* cassette excision. **b**, Table of expected PCR bands according to mutant. **c**, PCR bands obtained.

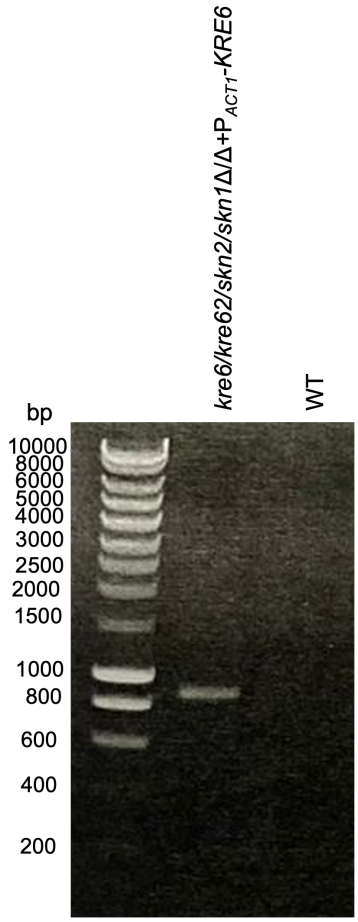

Figure S10: Control PCR of the quadruple mutant complemented for *KRE6* (*kre6/kre62/skn2/skn1*Δ/Δ+P$_{ACT1}$-*KRE6*)

KRE6 was reintegrated at the *RPS1* locus under the control of *ACT1* promoter, using *SAT1* as a selection marker.

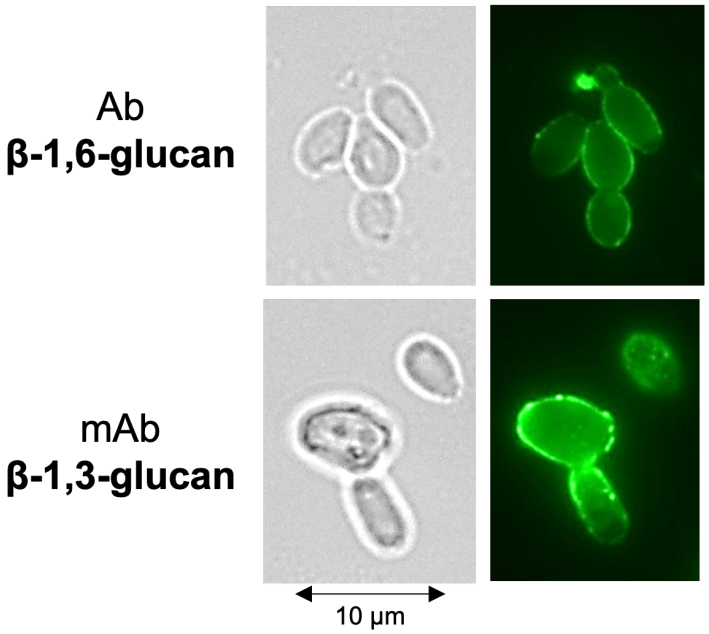

Figure S11: Exposure of β-1,6-glucans and β-1,3-glucans at the cell surface of *C. albicans* SC5314.

Cells were cultured in SD at 37°C. β-glucan exposure was detected by a polyclonal rabbit anti-β-1,6-glucan serum (top panel) and or monoclonal anti-β-1,3-glucan antibody (bottom panel).

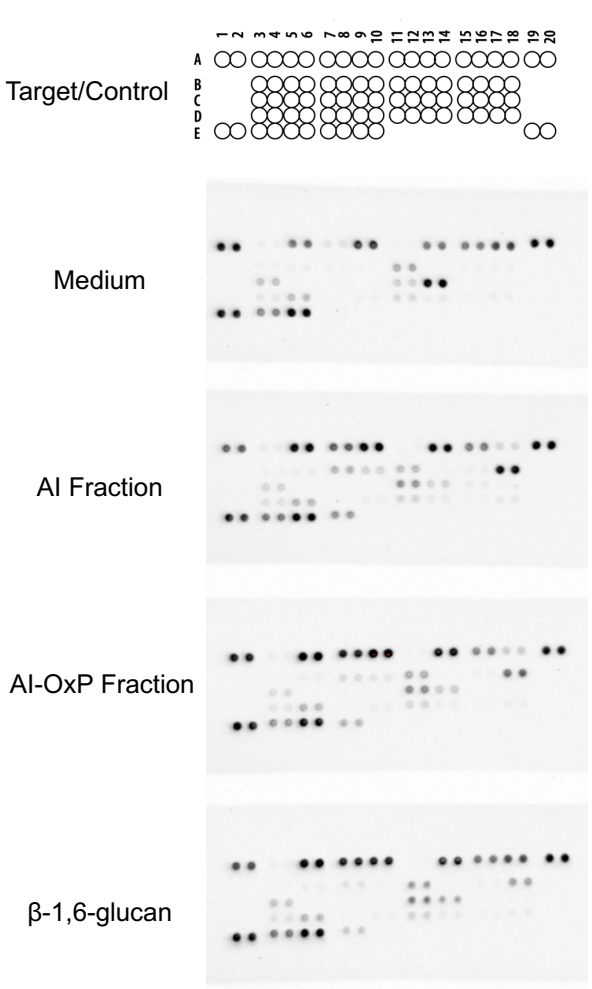

Target/Control	Coordinate		Target/Control	Coordinate
Reference Spots	A1, A2, A19, A20, E1, E2		IL-2	C5, C6
Negative Control	E19, E20		IL-4	C7, C8
CCL1/I-309	A3, A4		IL-5	C9, C10
CCL2/MCP-1	A5, A6		IL-6	C11, C12
MIP-1α / MIP-1β	A7, A8		IL-8	C13, C14
CCL5/RANTES	A9, A10		IL-10	C15, C16
CD40 Ligand /TNFSF5	A11, A12		IL-12 p70	C17, C18
Complement Component C5/C5a	A13, A14		IL-13	D3, D4
CXCL1/GR0α	A15, A16		IL-16	D5, D6
CXCL10/IP-10	A17, A18		IL-17A	D7, D8
CXCL11/I-TAC	B3, B4		IL-17E	D9, D10
CXCL12/SDF-1	B5, B6		IL-18/ IL-1F4	D11, D12
G-CSF	B7, B8		IL-21	D13, D14
GM-CSF	B9, B10		IL-27	D15, D16
ICAM-1/CD54	B11, B12		IL-32α	D17, D18
IFN-γ	B13, B14		MIF	E3, E4
IL-1α/IL-1F1	B15, B16		Serpin E1 /PAI-1	E5, E6
IL-1β/IL-1F2	B17, B18		TNF-α	E7, E8
IL-1ra/IL-1F3	C3, C4		TREM-1	E9, E10

Figure S12: Human proteome profiler done with culture supernatant from PBMCs stimulated with *C. albicans* cell wall fractions.

On the left, membrane blots obtained after incubation with supernatants from PBMCs cultures stimulated by different *C. albicans* cell wall fractions: AI, AI-OxP, β-1,6-glucans. Incubation with the culture medium was used as a control (top). On the right, coordinate of each protein (cytokines, chemokines, acute phase proteins) detected on the membranes. The experiment was performed once using a pool of 24 supernatants from the stimulation of PBMCs isolated from 8 healthy donors, each stimulated with 3 independent batches of fractions.

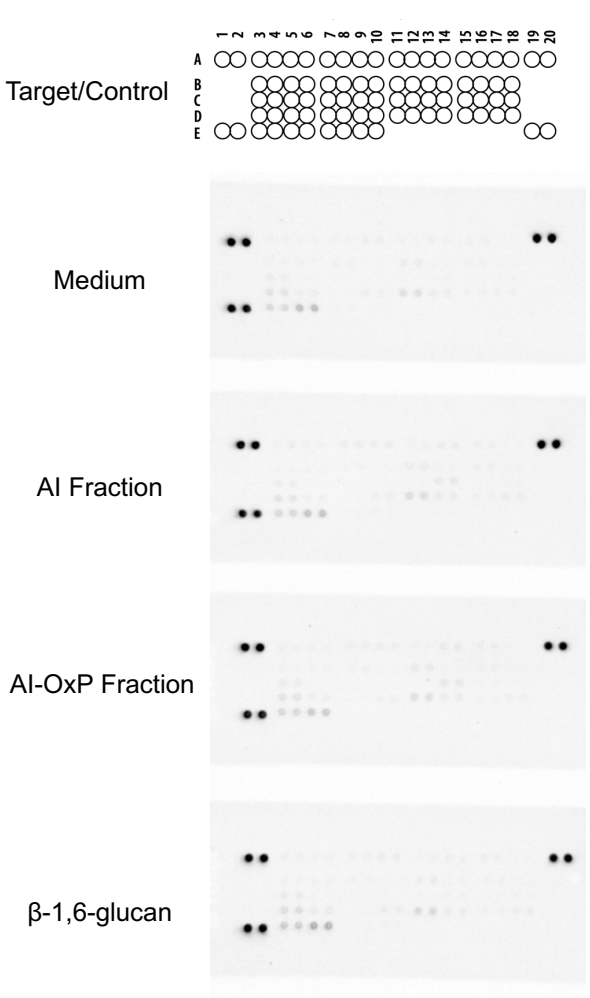

Target/Control	Coordinate		Target/Control	Coordinate
Reference Spots	A1, A2, A19, A20, E1, E2		IL-2	C5, C6
Negative Control	E19, E20		IL-4	C7, C8
CCL1/I-309	A3, A4		IL-5	C9, C10
CCL2/MCP-1	A5, A6		IL-6	C11, C12
MIP-1α / MIP-1β	A7, A8		IL-8	C13, C14
CCL5/RANTES	A9, A10		IL-10	C15, C16
CD40 Ligand /TNFSF5	A11, A12		IL-12 p70	C17, C18
Complement Component C5/C5a	A13, A14		IL-13	D3, D4
CXCL1/GR0α	A15, A16		IL-16	D5, D6
CXCL10/IP-10	A17, A18		IL-17A	D7, D8
CXCL11/I-TAC	B3, B4		IL-17E	D9, D10
CXCL12/SDF-1	B5, B6		IL-18/ IL-1F4	D11, D12
G-CSF	B7, B8		IL-21	D13, D14
GM-CSF	B9, B10		IL-27	D15, D16
ICAM-1/CD54	B11, B12		IL-32α	D17, D18
IFN-γ	B13, B14		MIF	E3, E4
IL-1α/IL-1F1	B15, B16		Serpin E1 /PAI-1	E5, E6
IL-1β/IL-1F2	B17, B18		TNF-α	E7, E8
IL-1ra/IL-1F3	C3, C4		TREM-1	E9, E10

Figure S13: Human proteome profiler done with culture supernatant from neutrophils stimulated with *C. albicans* cell wall fractions.

On the left, membrane blots obtained after incubation with supernatants from neutrophils cultures stimulated by different *C. albicans* cell wall fractions: AI, AI-OxP or β-1,6-glucans; incubation with the culture medium was used as a control (top). On the right, coordinate of each protein (cytokines, chemokines, acute phase proteins) detected on the membranes. The experiment was performed once using a pool of 24 supernatants from the stimulation of neutrophils isolated from 8 healthy donors, each stimulated with 3 independent batches of fractions.

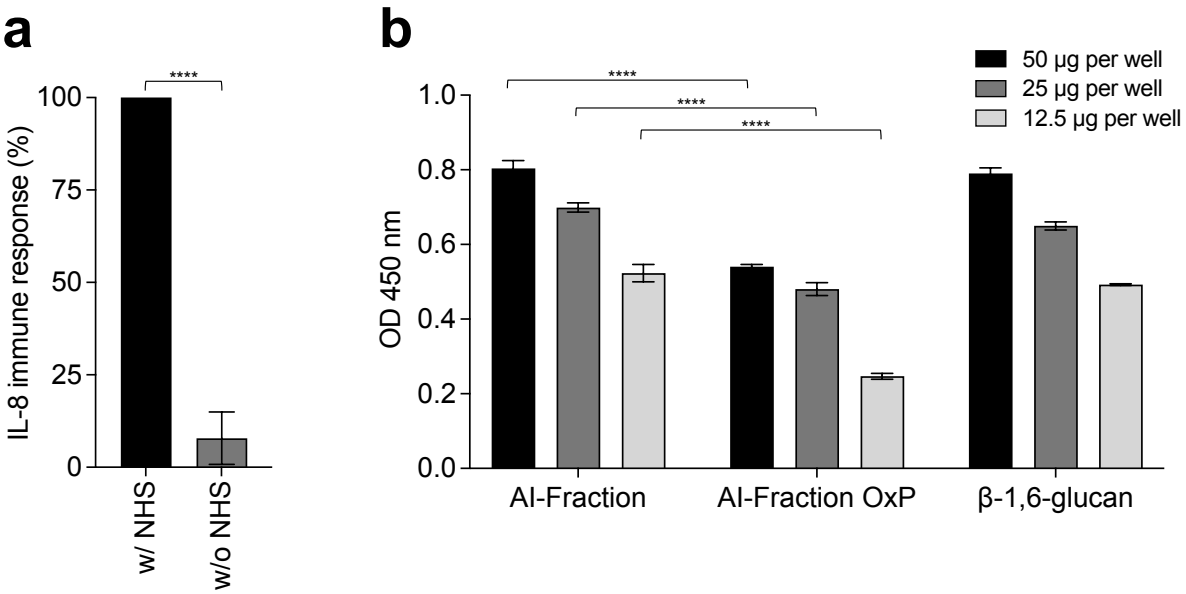

Figure S14: β-1,6-glucan from *C. albicans* activates complement system.

a, Normal human serum (NHS) enhances the immunostimulatory capacity of β-1,6-glucan from *C. albicans.* PBMCs isolated from healthy human donors (n=2) were stimulated with three independent batches of β-1,6-glucan at 25 µg/mL with (w/) or without (w/o) NHS (10%). Immune response was analyzed by measuring IL-8 released into the culture medium. Means are represented and data were analyzed with an unpaired parametric t-test: ****, $P < 0{,}0001$.

b, Complement factor C3b binds to β-1,6-glucan purified from *C. albicans* cell wall. Three cell wall fractions (AI, AI-OxP and β-1,6-glucan) from *C. albicans* were coated on microtiter plates at 50 µg, 25 µg or 12.5 µg per well. Human normal serum, diluted in Gelatin-Veronal Buffer (GVB), was added to activate complement pathways. The amount of deposited C3b on each fraction (=level on complement activation) was determined by using anti-human C3b and peroxidase-conjugated anti-mouse IgG antibodies. 3,3',5,5'-Tetramethylbenzidine (TMB) was used as the peroxidase substrate and the reaction was stopped with 4% H_2SO_4 and optical density (OD) was measured at 450 nm. The experiment was done with three independent batches of each cell wall fractions. Blank value was subtracted from the values presented. Statistical analyses were performed with one-way ANOVA with Tukey's multiple comparisons test: ****, $P < 0{,}0001$.

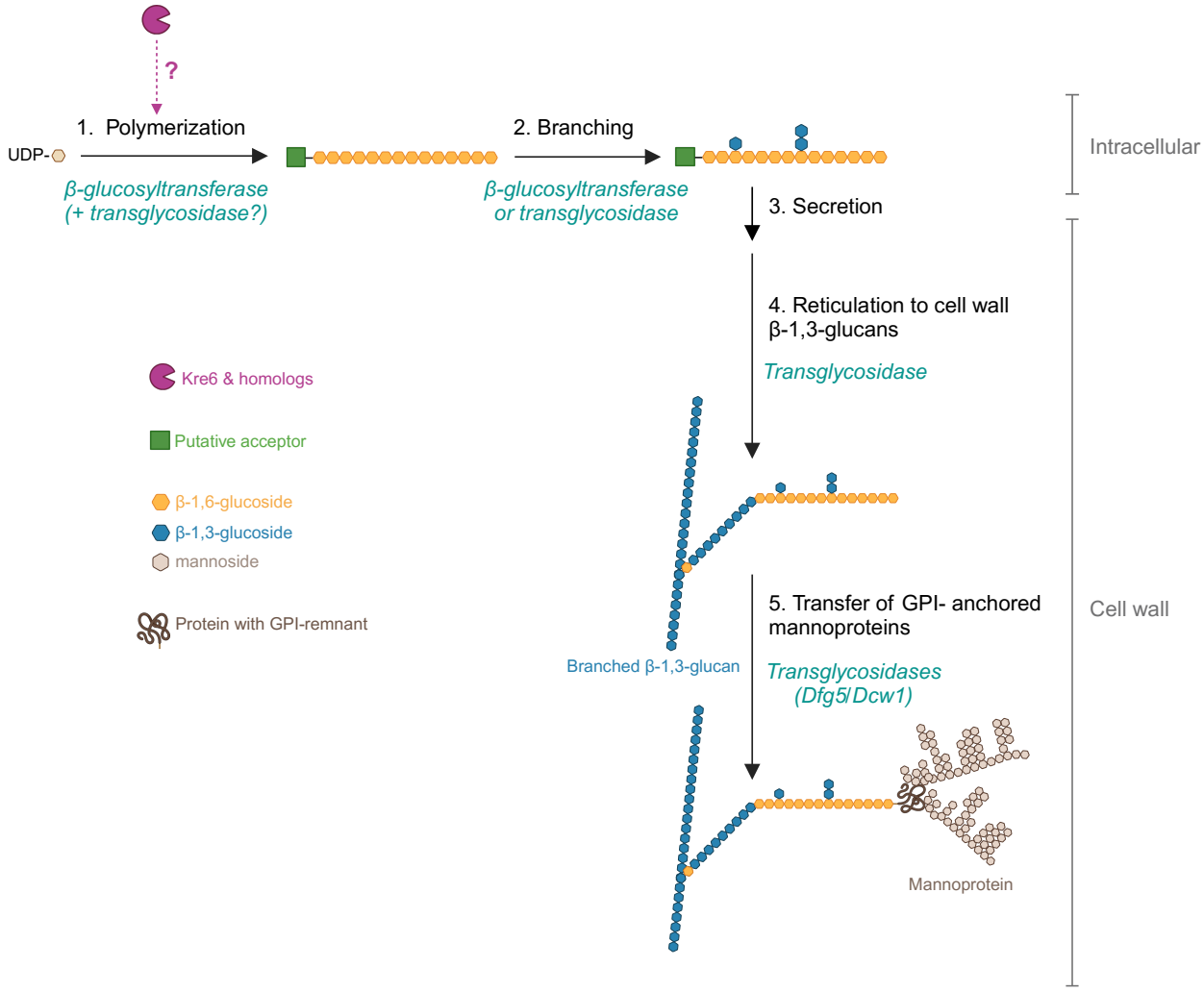

Figure S15: A model for β-1,6-glucan biosynthetic pathway and putative role of Kre6 family members in this process in yeast.

The cellular location of β-1,6-glucan synthesis in yeast is still unknown. We assume that synthesis begins intracellularly with the polymerisation of linear β-1,6-glucan chain (step 1), which requires a β-glucosyltransferase and UDP-glucose as a donor[33,92] and a putative acceptor (sugar, protein, lipid). Our data (Fig. 3g, S6) suggest that Kre6 and its homologues (Kre62, Skn1, Skn2) act at this stage, but their function remains unknown. Two proposed hypotheses are: 1) Kre6 family members are β-glucosyltransferases and 2) they have glycosylhydrolase and transglycosidase activity essential for polymerisation. Step 2 is the branching of nascent β-1,6-glucan where glucosides and laminaribiosides are added to form side chains. The enzymes (β-glucosyltransferase or transglycosidase) involved in this branching remain unknown. According to our data, members of the Kre6 family are not involved in branching (Fig. 3i). Next, the polysaccharide is secreted (step 3) and then cross-linked to β-1,3-glucans in the cell wall space by an unknown transglycosidase (step 4). The transfer of GPI-anchored proteins onto β-1,6-glucan (step 5), leading to the formation of the outer layer of the cell wall, appears to be driven by Dfg5/Dcw1[130]. The chronology between these two cross-links (Steps 4 and 5) has not been established.

Table S1: *C. albicans* strains used in this study.

Strain name	Parental strain	Relevant genotype	Reference
SC5314	-	Clinical blood isolate	PMID: 6394964
CAF2-1	SC5314	*URA3/ura3Δ::imm434*	PMID: 8349105
CAI4	CAF2-1	*ura3Δ::imm434/ura3Δ::imm434*	PMID: 8349105
BWP17	CAI4	*ura3Δ::imm434/ura3Δ::imm434 his1::hisG/his1::hisG arg4::hisG/arg4::hisG*	PMID: 10074081
SN152	CAI4	*arg4Δ/arg4Δ leu2Δ/leu2Δ his1Δ/his1Δ URA3/ura3Δ::imm434 IRO1/iro1Δ::imm434*	PMID: 15701792
cwh41Δ/Δ	CAI4	Same as CAI4 but *cwh41Δ::dp1200/cwh41Δ::dp1200 RPS1/rps1Δ::*Clp10	PMID: 17933909
rot2Δ/Δ	CAI4	Same as CAI4 but *rot2Δ::dp1200/rot2Δ::dp1200 RPS1/rps1Δ::*Clp10	PMID: 17933909
kre5Δ/Δ	SN152	Same as SN152 but *kre5Δ::leu2/kre5Δ::his1*	PMID: 20543849
kre6Δ/Δ	SC5314	*kre6Δ::HygB/kre6Δ::HygB*	This study
kre62Δ/Δ	SC5314	*kre62Δ::FRT/kre62Δ::FRT*	This study
skn2Δ/Δ	SC5314	*skn2Δ::FRT/skn2Δ::FRT*	This study
skn1Δ/Δ	SC5314	*skn1Δ::FRT/skn1Δ::FRT*	This study
kre6/skn1Δ/Δ	*kre6Δ/Δ*	*kre6Δ::HygB/kre6Δ::HygB skn1Δ::FRT/skn1Δ::FRT*	This study
kre6/kre62/skn2/skn1Δ/Δ	*kre6Δ/Δ*	*kre6Δ::HygB/kre6Δ::HygB kre62Δ::FRT/kre62Δ::FRT skn2Δ::FRT/skn2Δ::FRT skn1Δ::FRT/skn1Δ::FRT*	This study
kre6/kre62/skn2/skn1Δ/Δ+ P_{ACT1}*-KRE6*	*kre6/kre62/skn2/skn1Δ/Δ*	*kre6Δ::HygB/kre6Δ::HygB kre62Δ::FRT/kre62Δ::FRT skn2Δ::FRT/skn2Δ::FRT skn1Δ::FRT/skn1Δ::FRT RPS1/RPS1::*Clp*SAT1-*P_{ACT1}*-KRE6*	This study
kre1Δ/Δ	BWP17	Same as BWP17 but *kre1Δ::arg4/kre1Δ::his1*	Provided by Mathias Richard

P_{MRP1}-*CHS1/chs1*Δ	CAI4	Same as CAI4 but *chs1*Δ*::hisG/chs1*Δ:pSK-*URA3*-P_{MRP1}-*CHS1*	PMID: 11251855
*chs2*Δ/Δ	CAF2-1	Same as CAF2-1 but *chs2*Δ*::hisG/chs2*Δ*::hisG-URA3-hisG*	PMID: 8636047
*chs3*Δ/Δ	CAF2-1	Same as CAF2-1 but *chs3-2::hisG/chs3-3::hisG-URA3-hisG*	PMID: 7479842
*mnt1/mnt2*Δ/Δ	CAI4	Same as CAF2-1 but *mnt1-mnt2*Δ*::hisG/mnt1-mnt2*Δ*::hisG-URA3-hisG*	PMID: 15519997
*mnn2/22/21/23/24/26*Δ/Δ	CAI4	Same as CAF2-1 but *mnn2*Δ*::dpl200/mnn2*Δ*::dpl200 mnn22*Δ*::dpl200/mnn2*Δ*::dpl200 mnn23*Δ*::dpl200/mnn23*Δ*::dpl200 mnn24*Δ*::dpl200/mnn24*Δ*::dpl200 mnn26*Δ*::dpl200/mnn26*Δ*::dpl200 mnn21*Δ*::dpl200/mnn21*Δ*::dpl200*	PMID: 23633946
*mnn9*Δ/Δ	CAI4	Same *as CAF2-1 mnn9*Δ*::hisG/mnn9*Δ*::hisG* Δ*ura3*Δ*::imm434/ura3*Δ*::imm434*	PMID: 10601199
*och1*Δ/Δ	SN152	Same as SN152 but *och1*Δ*::leu2/och1*Δ*::his1*	PMID: 20543849
*fks1*Δ	SC5314	SC5314, but *fks1/fks1*Δ	PMID: 30370375
*phr1*Δ/Δ	BWP17	Same as BWP17 but *phr1*Δ*::hisG/phr1*Δ	PMID: 7823929
*phr2*Δ/Δ	BWP17	Same as BWP17 but *phr2*Δ*::hisG/phr2*Δ*::hisG-URA3-hisG*	PMID: 9315654

Table S2: ^{1}H and ^{13}C NMR resonance assignments, $^{3}J_{H1/H2}$ and $^{1}J_{H1/C1}$ coupling constants of the monosaccharide residues of cell wall β-1,6-glucan purified from the AI fraction.

Chemical shifts are expressed in ppm and coupling constants in Hz.

Residue	H1, C1 $^{3}J_{H1/H2}$, $^{1}J_{H1/C1}$	H2, C2	H3, C3	H4, C4	H5, C5	H6-H6', C6
-6)-β-Glc-(1,6)-	4.486 105.88 7.9 Hz 162 Hz	3.300 76.00	3.469 78.57	3.428 72.52	3.599 77.85	4.184-3.822 71.81
-3,6)-β-Glc-(1,6)-	4.519 105.63 7.8 Hz 162 Hz	3.498 75.71	3.707 87.46	3.544 71.07	3.627 77.52	4.191-3.838 71.81
β-Glc-(1,3)-	4.701 105.77 7.9 Hz 163 Hz	3.329 76.43	3.492 78.5	3.379 72.55	3.446 78.92	3.883-3.690 63.71

Table S3: Primers used in this study.

Primer name	Sequence (5' -> 3')	Remarks
SNR52/F	AAGAAAGAAAGAAAACCAGGAGTGAA	Forward primer for the amplification of SNR52 promoter (Min 2016)
sgRNA/R	ACAAATATTTAAACTCGGGACCTGG	Reverse primer for the amplification of sgRNA scaffold (Min 2016)
SNR52/N	GCGGCCGCAAGTGATTAGACT	Forward and reverse primers for nested PCR (for construction of sgRNA expression cassette; Min 2016)
sgRNA/N	GCAGCTCAGTGATTAAGAGTAAAGATGG	
CaCas9/F	ATCTCATTAGATTTGGAACTTGTGGGTT	Forward primer for amplifying the CaCas9 cassette (Min 2016)
CaCas9/R	TTCGAGCGTCCCAAAACCTTCT	Reverse primer for amplifying the CaCas9 cassette (Min 2016)
SNR52/R/SKN1	CGAGTCATTTCGTCTTGGTTCAAATTAAAAATAGTTTACGCAAGTC	Reverse primers for the amplification of SNR52 promoter with overlapping guide sequence of the target gene. Guide sequence in red.
SNR52/R/SKN2	TTCGATTCTAGCAACAGACTCAAATTAAAAATAGTTTACGCAAGTC	
SNR52/R/KRE62	GATATATTACTTGAATCACTCAAATTAAAAATAGTTTACGCAAGTC	
SNR52/R/KRE6	CTATAAGCTTGGAATGGTTTCAAATTAAAAATAGTTTACGCAAGTC	
sgRNA/F/SKN1	AACCAAGACGAAATGACTCGGTTTTAGAGCTAGAAATAGCAAGTTAAA	Forward primers for the amplification of sgRNA scaffold with overlapping guide sequence of the target gene. Guide sequence in red.
sgRNA/F/SKN2	AGTCTGTTGCTAGAATCGAAGTTTTAGAGCTAGAAATAGCAAGTTAAA	
sgRNA/F/KRE62	AGTGATTCAAGTAATATATCGTTTTAGAGCTAGAAATAGCAAGTTAAA	
sgRNA/F/KRE6	AAACCATTCCAAGCTTATAGGTTTTAGAGCTAGAAATAGCAAGTTAAA	

SAT1FLP/F/SKN1	ACTACCACTACTATTATAGAAATTTTTATCATA TATATACAATTGGCTACTAAAAACTTAAA CTTTTAATACAACTTACAGTACCGGGCCCCC CCTCGA	Primers to amplify the repair template (*SAT1*-Flipper or HygR)
SAT1FLP/F/SKN2	ATAATAGATTTTGTTTTTAAACGGATAACCCT TCCATTCCATTCTAGCAAACCAAAAGTAAA TCAAAAGAACTAACTACCGTACCGGGCCCCC CCTCGA	
SAT1FLP/F/KRE62	AATATTCAACAACTATTCTTTCTACTTCTTTTA AAGAACCCGAACTTTTTTTTTGACTTTATAA TAATTAATGTATCATTGTACCGGGCCCCCCC TCGA	
HygR/F/KRE6	GATAAGACCTCAAAATGGCGTCTCAAAGAGA GATGGAATGAATGGGATGAATCATCAAACAA GAG	
SAT1FLP/R/SKN1	AATTATATACAATGAATGAATGAATGAAAATG TCTATTTAAAAGTATATAAAAATATG TAAATATAGGGGGGTTGGTGTTGGCCGCTCT AGAACTAGTGGAT	
SAT1FLP/R/SKN2	CAGAGAACACATGAAGGGTGGTAAACTATTT TGTCAGTTTTTTTTCTCCTTTTTTTTAGT ACGTGGAGTTCGCCTTTAATGGCCGCTCTAG AACTAGTGGAT	
SAT1FLP/R/KRE62	ATCGTCTTGTTTGAGATTGTTCTTTTAACTTTT GTTCTACACTACCACCACCACCACCATC ATTGTTATTCTTGTTGTTGGGCCGCTCTAGAA CTAGTGGAT	
hygR/R/KRE6	AGTAGTAGTAGTAATAGTAGTACCATCGCCA CCTGACGTCGTATAGTGCTTGCTGTTCG	
Flanking_F/SKN1	CTACAGTTTATAGAAGTTAATACCAGTACC	
Flanking_F/SKN2	ATATCCCGCTCCATCCATTC	
Flanking_F/KRE62	AGGCTAGGCTAAGTATTAAC	
Flanking_R/SKN1	CATTATCATCAGGTCAATTTGACTCAT	
Flanking_R/SKN2	ACCACTGTCGTACAAAATTGC	
Flanking_R/KRE62	ATTACCTGATTTGGTGATGC	
screenKre6/F	ACTTGGCAACATTTGCAACA	
screenKre6/R	TCTGGGGTCACTTTCTTAAAATCCT	
ClpUL	ATACTACTGAAAATTTCCTGACTTTC	
ClpSAT	CTAGTGGATCCCCCAGATCATTATCC	
KRE6-FWD	GGGGACAAGTTTGTACAAAAAAGCAGGCTtgA TGGCGTCTCAAAGAGATTTAACTTCAAAT	Primers used for cloning KRE6 in pDONR207

KRE6-REV	GGGGACCACTTTGTACAAGAAAGCTGGGTcT TAACATCCAATTAAACTATTTTTAGGGAA	